

**Molecular characterization of a ribosome-inactivating protein from  
*Momordica* sp: literature survey and bioinformatics analysis**

**By**

**Karamjeet Kaur**

**(Bachelors' of Biotechnology)**

**Health Science Building**

**College of Medicine and Public Health**

**Flinders University, South Australia**

**A thesis Submitted in fulfilment of the requirement for the degree of**

**Masters of Biotechnology Studies**

**Flinders University**

**June, 2018**

# TABLE OF CONTENT

List of figure .....	5-6
List of table .....	7-8
Abstract .....	9-10
Acknowledgement .....	11
List of abbreviations .....	12
Table of amino acids .....	13
Chapter 1: Introduction .....	14
1.1 Introduction .....	15-16
1.2 Ribosome-inactivating protein (RIPs) .....	16-17
1.3 Types of RIPs .....	17-18
Chapter 2: Review of literature .....	19
2.1 Ribosome-inactivating protein in plants .....	20
2.2 Enzyme like activities of ribosome-inactivating protein .....	21
2.2.1 DNase activity of RIPs .....	21
2.3 N-glycosidase activity of RIPs .....	21-23
2.4 Therapeutic activities of ribosome-inactivating protein .....	24
2.4.1 Antitumor activity of RIPs .....	24-25
2.4.2 Antiviral activity of RIPs .....	26-27
2.4.3 Antifungal activity of RIPs .....	28-29
2.4.4 Antimicrobial activity of RIPs .....	30
2.4.5 Insecticidal activity of RIPs .....	31-32
2.5 Structure function relationship of type-1 RIPs .....	33
2.5.1 The structure of Ricin .....	33
2.5.2 The structure of MAP30 .....	34

<b>Chapter 3: Materials and method .....</b>	<b>35</b>
<b>3.1 Ribosome-inactivating protein extraction outline .....</b>	<b>36</b>
<b>3.3 Materials .....</b>	<b>37</b>
<b>3.3.1 Extraction of RIPs from <i>Momordica balsamina</i> .....</b>	<b>37</b>
<b>3.3.2 Ammonium sulphate precipitation .....</b>	<b>37</b>
<b>3.3.3 Estimation of protein .....</b>	<b>38</b>
<b>3.3.4 Ion-exchange chromatography .....</b>	<b>38</b>
<b>3.3.5 SDS-PAGE gel electrophoresis .....</b>	<b>39-40</b>
<b>3.3.6 Concentrations of proteins .....</b>	<b>40-41</b>
<b>3.3.7 DNase like activity of balsamin .....</b>	<b>41</b>
<b>3.3.8 Bioinformatics analysis .....</b>	<b>41</b>
<b>3.3.9 Amino acid sequence .....</b>	<b>41</b>
<b>3.3.10. Building three dimensional model of Alpha-MMC.....</b>	<b>42</b>
<b>Chapter 4: Results and discussion .....</b>	<b>43</b>
<b>4.1 Morphological studies .....</b>	<b>44</b>
<b>4.2 Purification of balsamin .....</b>	<b>45</b>
<b>4.2.1 Ammonium sulphate precipitation .....</b>	<b>45</b>
<b>4.2.2 Ion-exchange chromatography .....</b>	<b>46-47</b>
<b>4.2.3 SDS-PAGE gel electrophoresis of chromatography fraction .....</b>	<b>47-48</b>
<b>4.2.4 DNase-like activity of balsamin .....</b>	<b>48-49</b>

<b>4.3 Bioinformatics analysis of balsamin .....</b>	<b>50</b>
4.3.1 Prediction of biophysical and physiochemical parameters of protein .....	51
4.3.2 Protein identification with RIPs type-1 .....	52
<b>4.4 Sequence alignment .....</b>	<b>53</b>
4.4.1 Sequence alignment of balsamin .....	53-54
<b>4.5 Phylogenetic analysis.....</b>	<b>55</b>
<b>4.6 Building a three-dimensional of Alpha-MMC .....</b>	<b>56-57</b>
<b>4.7 Assessment of the model with Ramachandran plot .....</b>	<b>58</b>
<b>4.8 Discussion .....</b>	<b>59-60</b>
<b>Conclusion .....</b>	<b>61-62</b>
<b>Future prospective .....</b>	<b>62</b>
<b>References .....</b>	<b>63-70</b>
<b>Appendix .....</b>	<b>71-73</b>

# LIST OF FIGURES

<b>Figure 2.1:</b> The detection method of Ricin with relation to biological steps which occur during Ricin intoxication .....	23
<b>Figure 2.2:</b> The ribbon diagram of Ricin reproduced from Protein Data Bank ( <a href="http://www.pdb.org">www.pdb.org</a> ) .....	33
<b>Figure 2.3:</b> The ribbon structure of MAP30 reproduced from <a href="http://www.pdb.org">www.pdb.org</a> from Protein Data Bank .....	34
<b>Figure 3.1:</b> The schematic presentation of protein extraction .....	36
<b>Figure 4.1:</b> Different stages of <i>Momordica balsamina</i> .....	45
<b>Figure 4.2:</b> SDS-PAGE analysis of Ammonium sulphate precipitation. ....	46
<b>Figure 4.3:</b> Profile of Ion-exchange chromatography of CM-Sepharose. ....	47
<b>Figure 4.4:</b> SDS-PAGE analysis of ion-exchange chromatography fraction. ....	48
<b>Figure 4.5:</b> Agarose gel electrophoresis exhibiting DNase-like activity of balsamin .....	49
<b>Figure 4.6:</b> The amino acid sequence alignment of balsamin with other types of ribosome-inactivating proteins (RIPs) from plants .....	54
<b>Figure 4.7:</b> Molecular Phylogenetic analysis by Maximum Likelihood method .....	55
<b>Figure 4.8:</b> The three dimensional structure of alpha momorcharin (4yp2.1.A) was used as a template to construct SWISS-MODEL.....	57

**Figure 4.9:** Ramachandran plot of balsamin. .... 58

# LIST OF TABLES

<b>Table 1:</b> Table of amino acids .....	13
<b>Table 2.1:</b> The different types of RIPs with antitumor activity .....	25
<b>Table 2.2:</b> Different types of RIPs with antiviral activities .....	27
<b>Table 2.3:</b> overview of different types of RIPs with antifungal activity .....	29
<b>Table 2.4:</b> overview of different types of RIPs with antimicrobial activity .....	30
<b>Table 2.5:</b> insecticidal activity of different types of RIPs .....	32
<b>Table 3.1:</b> The concentrations of reagents were used to prepare the 12% separating gel and 4% stacking gel .....	77
<b>Table 3.3:</b> The Concentration of protein using Ammonium sulphate precipitation (mg/ml) is performed with Bradford assay .....	78
<b>Table 4.1:</b> The predicted biophysical and physiochemical parameters of balsamin were done with PROTPARAM .....	51
<b>Table 4.2</b> Protein sequences from NCBI database was performed with BLAST program .....	52
<b>Table 4.3:</b> The list of amino acids present in each species of ribosome-inactivating protein .....	79
<b>Table 4.4:</b> The model built with SWIIS-MODLE with Alpha-MMC as template used to build it with their oligo-state, ligand and QMEAN score .....	56
<b>Table 4.5:</b> The pseudo-energies of the predicted balsamin model with their Z score energy.....	57
<b>Table 3.4:</b> The concentration of protein in ammonium precipitation was performed with Bradford assay and the standard curve was used to determine the yield of protein in each sample. The 60%	

ammonium precipitation has the highest protein yield however the 20% has the lowest protein yield ..... 73

**Table 3.5:** Various bioinformatics tools of used in this project ..... 73

## ABSTRACT

Plants are known to contain variety of secondary metabolites such as tannis, terpenoids, alkaloids, flavonoids and oil that exhibit therapeutic importance and are employed by herbalist/ naturopaths in the treatment of various ailments. A number of therapeutic proteins such as astragalins, fisetin, B-glucan and many more have been obtained through plant-based system and one such protein that naturally occurs in plant kingdom is ribosome-inactivating protein.

Ribosome inactivating proteins (RIPs) are ribotoxins with an N-glycosidase action that hydrolyses the N-glycosidic bond of adenine residue arranged in significantly loop structure of 28S rRNA. The selective toxicity of RIPs is the main reason to have primary focus of research has been the application of RIPs as the toxic agent in the carcinogenic applications. RIPs have been classified into three types on the basis of their physical structure and function. Type-1 RIPs has a single chain with the molecular weight 30 kDa, in type-2 RIPs subunits are linked by a disulfide bond; these types of proteins are heterodimeric proteins which have the ribosome-inactivity activity on separate polypeptides. Type-3 RIPs are produced as inactive single polypeptide protein with a molecular weight around 58 kDa contains a single polypeptide chain combined to zymogens are held for proteins.

Ribosome-inactivating proteins are most found in plant families such as *Cucurbitaceae*, *Caryophyllaceae*, *Eupobiaceae* and *Phytolaccaceae*. Majority of RIPs have been investigated from the family *Cucurbitaceae* to determine of their biological activities, like MAP30 from *Momordica charantia*, balsamin from *Momordica balsamin*, trichosanthin from *Trichosanthes kirilowii*, bryodin from *Bryonia dioica*, momorcharin from *Momordica charantia*.

*Momordica balsamina* is found in tropical region of Africa, North-part of India, Northern Territory Australia and Central America. It is also known as Balsam apple. It belongs to the *Cucurbitaceae* family that is tendril-bearing high climbing vine. All parts of this plant such as seeds, leaves, bark as well as the fruit contain various types of nutritional and medicinal components such as alkaloids, saponins, flavonoids, terpene and balsamin protein. The leaves of this plant used as a source of nutrient because they contain 17 amino acids while mineral composition such as magnesium, phosphorus, calcium, zinc, sodium, potassium etc. It also plays an important role in pharmaceuticals and most of the components of this plant are used as anti-cancer agents.

The phytochemical analysis of the balsamin revealed that it contains different varieties of secondary metabolites such as tannin, terpenoids, alkaloids, phenols that have been used for the treatment of various types of diseases. Balsamin was partially purified from the seeds of *Momordica balsamina*. The three dimensional (3D), structure of balsamin was predicted with SWISS-MODEL server while using  $\alpha$ -MMC as a template (a RIP obtained from *M. charantia*; RIP1\_MOMCH).

## Acknowledgement

I would like to express my thanks to my supervisor Associate Professor Munish Puri for his amazing and enlightening assistance supervising of this project and all the advice he has given me on conducting quality research. I would also like to thank you the Research Associate Dr Reinu Abraham for her guidance during writing my thesis.

I will always owe a great deal of gratitude towards Senior Laboratory Manager Ricardo Pinto Araujo for his support and guidance. I would also like to thank all the staff and students in the Department of Medical biotechnology for their assistance during my research project.

I would like to thank all PhD candidates who were willing to support me during my experiments and give me advice when I needed it, this help was really priceless.

I am also very grateful to my family and friends for supporting me throughout my project when I needed it the most during the difficult times I encountered throughout my research.

(Karamjeet kaur)

## List of Abbreviations

<b>RIPs</b>	<b>Ribosome-inactivating proteins</b>
<b>MAP30</b>	<b>Momordica antiviral protein</b>
<b>PAP</b>	<b>Pokeweed antiviral protein</b>
<b>Alpha-MMC</b>	<b>Alpha-momorcharin</b>
<b>PDB</b>	<b>Protein Data Bank</b>
<b>QMEAN</b>	<b>Qualitative model energy analysis</b>
<b>MbRIP-1</b>	<b><i>Momordica balsamina</i> ribosome-inactivating protein</b>
<b>GRAVY</b>	<b>Grand average of hydropathicity</b>
<b>E-value</b>	<b>Expect value</b>
<b>TEMED</b>	<b>Tetramethylethylenediamine</b>
<b>HBV</b>	<b>Hepatitis B Virus</b>

## Table of amino acids

<b>Ala</b>	<b>Alanine</b>
<b>Arg</b>	<b>Arginine</b>
<b>Asn</b>	<b>Asparagine</b>
<b>Asp</b>	<b>Aspartic acid</b>
<b>Cys</b>	<b>Cysteine</b>
<b>Glu</b>	<b>Glutamic acid</b>
<b>Gly</b>	<b>Glycine</b>
<b>His</b>	<b>Histidine</b>
<b>Ile</b>	<b>Isoeucine</b>
<b>Leu</b>	<b>Leucine</b>
<b>Lys</b>	<b>Lysine</b>
<b>Met</b>	<b>Methionine</b>
<b>Phe</b>	<b>Phenylalanine</b>
<b>Pro</b>	<b>Proline</b>
<b>Ser</b>	<b>Serine</b>
<b>Thr</b>	<b>Threonine</b>
<b>Trp</b>	<b>Tryptophan</b>
<b>Tyr</b>	<b>Tyrosine</b>
<b>Val</b>	<b>Valine</b>

# **Chapter 1:**

# **Introduction:**

## 1.1 INTRODUCTION

Plants are used to manufacture safe and effective therapeutic drugs. Some of the secondary metabolites which are produced by plants has the ability to inhibit cell division so that they can be used to treat various ailments (Buyel, 2018). From the data of Food and Drug Administration almost 40% molecules which are used in therapeutics drugs are from natural compounds, 74% are effective in the anti-cancer therapy (Seca and Pinto, 2018). For example, paclitaxel is antimicrotuble agent which is classified as plant alkaloid (secondary metabolite of plants) is used for the treatment of various types of cancers such as; breast cancer, lung cancer, cervical cancer, HIV, Hepatitis C, diabetes and pancreatic cancer (Frederico et al., 2017).

Many drugs derived from the natural products plays an important role in pharmaceuticals. Most of the compounds derived from plants are used as anti-cancer agents (Moloudizargari et al., 2013). Many natural products which are chemo preventive agents are able to inhibit carcinogenesis (Wang et al., 2016). The major pharmaceutical industries are showing their interest to manufacturing therapeutic drugs from plants with effective, safe and proved quality and quantity methods. Most of the anti-cancer drugs available in the market are derived from natural resources due to their less adverse effect compared with synthetic drugs (Abu-Darwish and Efferth, 2018). The uses of allopathic drugs results into various side effects therefore naturopaths prefer the use of medicinal plants to cure different types of diseases (Khan, 2014).

Several secondary metabolites of plants and their semi- synthetic derivatives are possessing therapeutic activity. It has been reported that natural products assumed the basic part of modern drug improvement, particularly for innovative treatment for various ailments (Veeresham, 2012). The biggest challenge to producing these kinds of therapeutic proteins is that they will be safe and economically can be adjusted to meet growing needs (Abu-Darwish and Efferth, 2018). Ribosome inactivating protein (RIPs) is that protein which is generally circulated in the plant kingdom and shows therapeutic and agricultural significance.

Some of the benefits of making the therapeutic drugs from plants are safe and cost effective. All alternative protein producing methods require clean working conditions for some period of time, however in plant based system it does not require (Ayrle et al., 2016).

Plants are used as a source of therapeutic agents because they contain different varieties of secondary metabolites such as tannin, terpenoids, alkaloids, phenols that have been used for the treatment of various types of diseases (Narsing Rao et al., 2017). A number of therapeutic proteins such as astragalins, fistein, B-glucan and many more have been reported through plant-based system. Furthermore, plants also contain particular proteins such as peroxidase, proteinase inhibitors, and chitinases (Stirpe et al., 1992). These types of proteins respond to bacterial, viral and various types of fungal infections and have been used for the treatment of different diseases such as cancer, HIV and Hepatitis C (Bolognesi et al., 2016).

Some selective proteins have been investigated to improve the plant defence against various pathogens, anticancer agents, antiviral and antibacterial agents with different kinds of biological and biochemical properties (Salehi et al., 2018). The proteins have toxicity which is known as ribosome-inactivating proteins. The majority of ribosome-inactivating proteins are found in plants but also in fungi and bacteria. RIPs are ribotoxins with an N-glycosidase action that inhibit translation through their activity against rRNA (Polito et al., 2016).

## **1.2 RIBOSOME-INACTIVATING PROTEINS**

Ribosome inactivating proteins (RIPs) are ribotoxins with an N-glycosidase action that hydrolyses the N-glycosidic bond of adenine residue arranged in significantly loop structure of 28S rRNA (Stirpe et al., 1992, Puri et al., 2012). This depurination inactivates the ribosome, thereby blocking its further participation in protein synthesis. Additionally, N-glycosidase activity, RIPs likewise has ribonuclease, DNase, DNA glycosidase, antimicrobial (Bolognesi et al., 2016). Ribosome inactivating proteins are generally dispersed among various plants, genera and inside a wide range of tissues. For plants, RIPs have been connected to protection by antiviral, antifungal, and insecticidal properties exhibited *in-vitro* and in transgenic plants.

These proteins also considered as extraordinary in the field of therapeutic on account of their exceptional natural activities towards animal and human cells (Polito et al., 2016).

MAP30 RIPs inhibits the production of the hepatitis B virus (HBV). The introduction HepG to MAP30 results in inhibition of HBV, DNA replication and HBsAg secretion. MAP30 is also shows to inhibit the expression of HBV antigen so the DNA viral replication decreases also reduce the synthesis of cDNA. Study shows that the high doses of MAP30 are effective in suppressing the viral replication by altering the kinetics of replicative DNA intermediates (Puri et al., 2012).

Balsamin from *Momordica balsamina*, MAP30 from *Momordica charantia*, alpha-MMC from *Momordica charantia*, is a type-1 RIPs. Balsam apple is also known by the botanically named *Momordica balsamina*. It belongs to the *Cucurbitaceae* family that is tendril-bearing high climbing vine (Zhang et al., 2014). All parts of this plant such as seeds, leaves, bark as well as the fruit contain various types of nutritional and medicinal components such as alkaloids, saponins, flavonoids, terpene and balsamin protein. The leaves of this plant used as a source of nutrient because they contain 17 amino acids while mineral composition such as magnesium, phosphorus, calcium, zinc, sodium, potassium etc (Seca and Pinto, 2018). It also plays an important role in pharmaceuticals and most of the components of this plant are used as anti-cancer agents. In Nigeria, the leaves of this plant were used by people to cook soup which was very beneficial for the lactating mothers and also helps them to purify their breast milk as well as helpful to regain the lost blood during the time of labour pain.

### 1.3 TYPES OF RIPs

Different RIPs have been reported from almost 50 plant species with covering 17 families such as *Cucurbitaceae*, *Euphorbiaceae*, and *Poaceae* (Sharma et al., 2004b). Number of evidences shows that RIPs have been purified from fungi, for example, *Aspergillus restrictus*, *Aspergillus fumigatus* and bacterial strains like *shigella dysenteria*. There has been no evidence that demonstrates the presence of RIPs in animals (Hamilton et al., 2016).

Ribosome inactivating proteins (RIPs) are divided into 3 types on the basis of their structure and function such as type-1 RIPs, type-2 RIPs and type-3 RIPs.

Type-1 RIPs, additionally called Halo RIPs consist of the single polypeptide chain with an molecular weight range from 26-35 kDa. These RIPs are known to have RNA *N*-glycosidase activity (Puri et al., 2012).

Type-2 RIPs has the molecular weight of 60-65 kDa. These type of proteins are used as anti-cancer agents (Vitetta et al., 1987). It comprise of two polypeptide chains where A-chain displays *N*-glycosidase action, B-chain binds to particular galactose (Ng et al., 2010). Type-2 RIPs are highly toxic heterodimeric protein with various enzymatic activity and lectin activities in separate polypeptide subunits (Narsing Rao et al., 2017).

Type-3 RIPs with a molecular weight around 58 kDa contains a single polypeptide chain combined to zymogens are held for proteins. These are fundamentally and transformative, identified with a jasmonate initiated protein. Type-3 RIPs have been isolated from maize, barley and sorghum (Mak et al., 2007). This type of protein is found in roots, leaves and often accumulates in seeds. Type-3 RIPs has biological activities towards animal and human cells. It is used to protect plants from different bacterial pathogens, viruses and fungi, and are also called as antiviral protein (AVP's) (Bibi et al., 2011).

RIPs are concentrated on medicinal and therapeutic applications to assess their potential use as toxins in the treatment of different human diseases (Cole et al., 2011). Some types of RIPs have appeared to display antiviral action against infections contaminating plants and people. Late enthusiasm for RIPs has been developing because of their antiviral exercises (Puri et al., 2009). Ribosome-inactivating proteins show antitumor activity.

The present study was carried out in view of the biochemically characterization of ribosome-inactivating protein from *Momordica* sp: The following objectives of the study were achieved:

- Partial purification of balsamin from the seeds of *Momordica balsamina*.
- Functional characterization and bioinformatics studies of balsamin.

# Chapter 2:

## Review of Literature:

A number of therapeutic proteins such as astragalin, fisetin, B-glucan and many more have been obtained from plant-based system; one class of that naturally occurs in plant kingdom is ribosome-inactivating protein. Ribosome-inactivating protein is found in fungi, bacteria and majority of

these proteins are found in plant kingdom. RIPs are *N*-glycosidase which is specifically used to remove particular purine residues from the Sarcin/ricin (S/R) loop of large ribosomal subunit.

## **2.1 RIBOSOME-INACTIVATING PROTEINS IN PLANTS**

Ribosome-inactivating proteins of higher plants have been purified and characterized from different plant kingdom. RIPs are a group of protein that inhibit protein synthesis in eukaryotic and prokaryotic cells (Sharma et al., 2004b). The process of inhibition of protein is done because the *N*-glycosidase depurination of rRNA at conserved residues. Ribosome-inactivating proteins (RIPs) are ribotoxins with an *N*-glycosidase action that hydrolyses the *N*-glycosidic bond of adenine residue arranged in significantly loop structure of 28S rRNA (Stirpe et al., 1992).

RIPs are distributed among the plant genera spanning 50 species and 14 families such as *Cucurbitaceae*, *Poaceae*, *Euphorbiaceae* and *phytolaccaceae*. All types of RIPs are localized to seeds, leaves and roots of plants. Type-1 ribosome-inactivating proteins are mostly abundant protein that is mainly found in plants (Stirpe et al., 1992). The first, type-1 ribosome-inactivating proteins was Pokeweed antiviral protein (PAP) from *Phytolacca Americana* followed by momordin from *Momordica charantia*, luffin from *Luffa cylindrical*, bryodin from *Bryonia dioica*, dianthin from *Diathus caryophyllus*, trichosanthin from *Trichosanthes kirilowii*,  $\alpha$ -momorcharin and  $\beta$ -momorcharin from *Momordica charantia* and saporin from *Saponaria officinalis* (Kaur et al., 2012).

All types of RIPs have been reported to investigate their potential usages in *Cucurbitaceae* such as trichosanthin and trichokirin (*Trichosanthes kirilowii*), bryodin (*Bryonia dioica*), luffin (*Luffa cylindrica*) and momorcharin (*Momordica charantia*) (Kaur et al., 2012). There is more possibility that the RIPs from the same plants have similarities in the structure and physiochemical properties with same amino acid sequences (Ajji et al., 2018). In some part of plants (*Momordica charantia*), seeds contain multiform of type-1 RIPs such as alpha and beta momorcharin, MAP30,  $\gamma$ -momorcharin,  $\delta$ -momorcharin and  $\epsilon$ -momorcharin and charantia are discovered (Puri et al., 2009).

## **2.2 VARIOUS ACTIVITIES OF RIBOSOME-INACTIVATING PROTEIN**

### **2.2 ENZYME LIKE FUNCTION**

#### **2.2.1 DNase activity**

The DNase activity is proposed with an alternative mechanism of cytotoxicity for type-1 RIPs and type-2 RIPs. There are all types of RIPs which were prepared to analyse their non-specific depurination and DNase activity (Akkouh et al., 2015). The DNase activity associated with RIPs is because of their non-specific depurination of DNA with subsequently hydrolysis through contaminating nuclease (Nicolas et al., 1997). DNase activity with type-1 RIPs, for example: pokeweed antiviral protein (PAP) and with type-2 RIPs, in Ricin due to their nuclease contamination.

There are number of Ribosome-inactivating proteins, which have been analysed to divide super coiled DNA to linearize single stranded DNA (Ajjji et al., 2016). Trichosanthin shows DNase movement towards super coiled DNA *in-vitro* (Gerl and Vaux, 2005). It was observed that Trichosanthin can linearize super coiled and relaxed circular DNA. Trichosanthin is isolated from Chinese therapeutic herb *Trichosanthes kirilowii* (Shu et al., 2009). It is a type-1 ribosome-inactivating protein with the highest mode of action towards tumour cells.

### **2.2.2 N-glycosidase activity**

The first enzymatic activity of ribosome-inactivating proteins were isolated in Ricin (Giansanti et al., 2010). Ricin is a type-2 ribosome-inactivating protein. It consists of two-polypeptide chain. These both polypeptide chains are joined by single disulphide bond. This protein removes a single adenine residue at position 4324 in 28S rRNA of rat liver ribosome that defines RIPs as ribosome specific N-glycosidase. The mechanism is divided into two steps (Fermani et al., 2009).

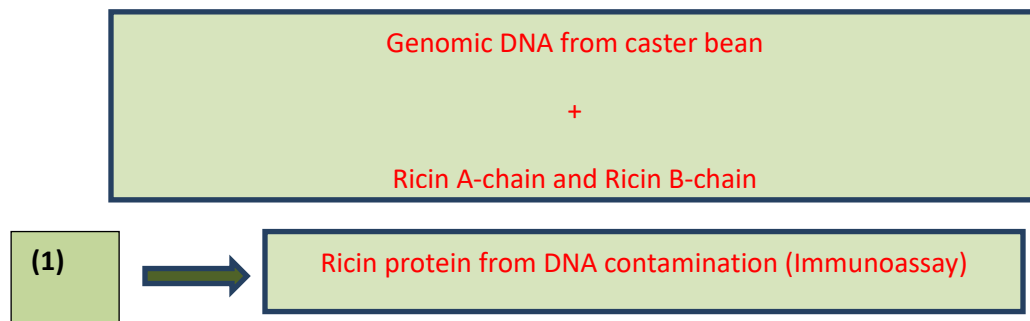
The first step is the involvement of recognition of highly conserved GAGA region in the stem loop region and depurination of adenine from the sequence. This step is important for the interaction with ribosome-elongation factor (May et al., 1989). In the second step, the  $\beta$ -elimination cleaves the 3' end of rRNA. Ricin has the ability to depurination of the ribosome from yeast and animals, however; it does not show any activity towards *E.coli* and plant ribosome (Das et al., 2011).

Furthermore, alpha-MMC from *Momordica charantia* shows the high specificity towards eukaryotic ribosome. It acts only on 28s rRNA to release Endo's fragment (Endo et al., 1987). The detection methods of Ricin are discussed in Figure 2.1. The process is divided into three stages.

In the first stage, the contamination of DNA and Ricin protein can be detected by immune-based assay, mass spectroscopy and qPCR techniques (Nicolas et al., 1997).

The second stage is depurination and ribosome inhibition. In this stage the different types of assays can be used to monitor the inhibition of protein translation and detect ribosome inactivation by Ricin (Giansanti et al., 2010).

The third stage is apoptosis and cell death. In this stage, cytotoxicity assay can be used to detect Ricin triggered cell death. The X-ray structure of Ricin can be generated with the help of PyMol software (Endo et al., 1987).



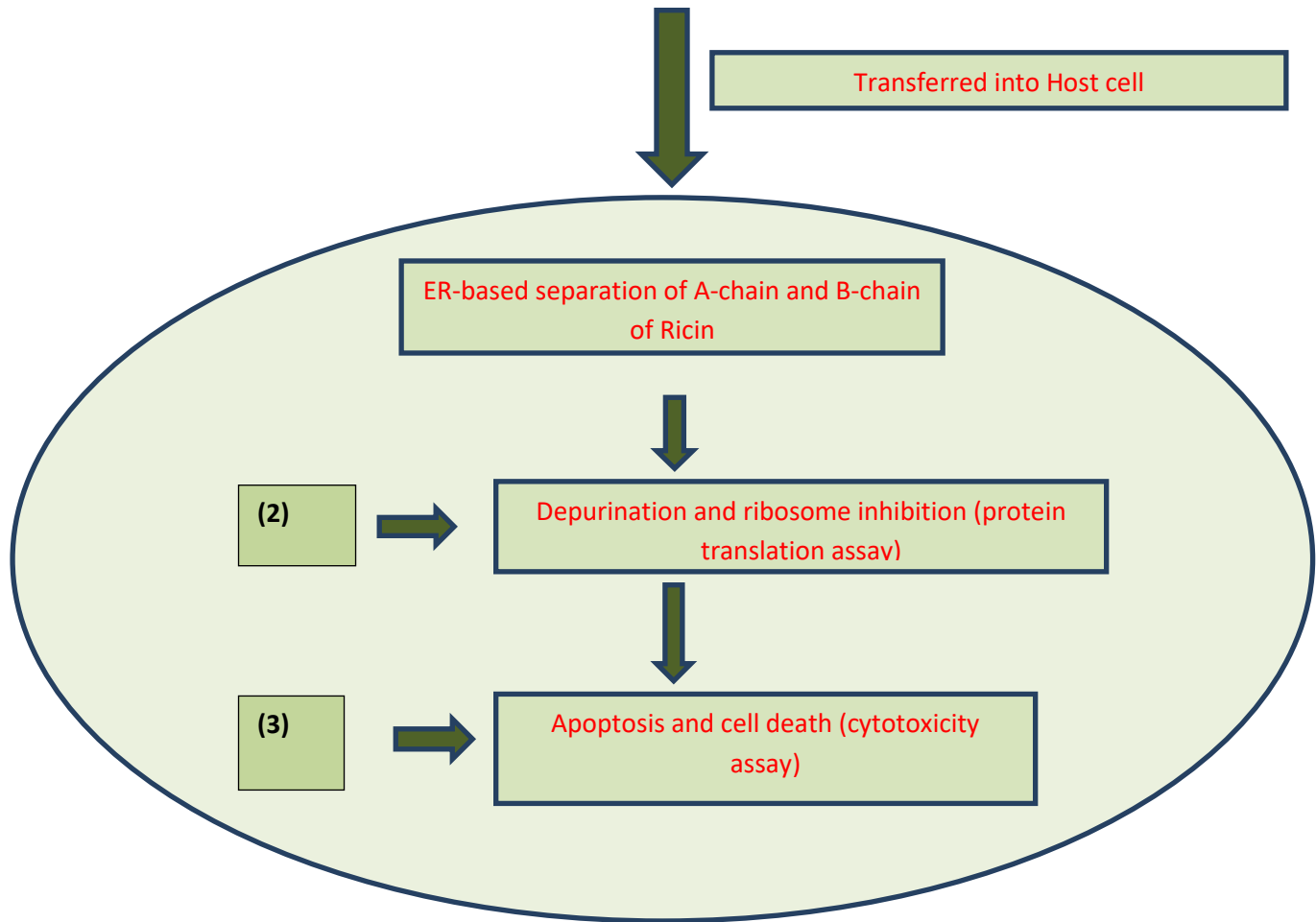


**Figure 2.1:** The detection method of Ricin with relation to biological steps which occur during Ricin intoxication. The diagram was reproduced from (Endo et al., 1987)

## 2.3 THERAPEUTIC ACTIVITIES OF RIBOSOME-INACTIVATING PROTEINS

### 2.3.1 Antitumor activity of RIPs against the breast cancer cells

Ribosome-inactivating proteins have shown *in-vitro* and *in-vivo* antitumor activity as described in Table 2.1. The anti-cancer activities of RIPs are characterized to apoptosis pathway (Pucci et al., 2000). For example, MAP30 induces apoptosis in liver cancer cells via activation of both the

caspase 8-regulated extrinsic and caspase-9-regulated intrinsic apoptotic cascade (Gerl and Vaux, 2005). Apoptosis can be induced by different types of pathways such as stress induced mitochondrial pathway, ribotoxic stress response and down regulation of anti-apoptotic factors like Mcl-1, NAD<sup>+</sup> depletion by DNA damage (Zeng et al., 2015). Due to their sufficient level of cytotoxicity, RIPs are considered as a potential biological agent for the cancer therapy (Pizzo and Di Maro, 2016). There are three types of RIPs isolated from *Momordica charantia* such as MAP30, MAC30, and Alpha-MAC (Xiong et al., 2009).

MAP30, a 30 kDa single stranded RIPs show antitumor activity against various human cancer cell lines such as Brain glioblastoma, breast carcinoma, epidermis carcinoma, liver hematoma and myeloma neuroblastoma (Leung et al., 1987). MAP30 can induce the cell growth arresting in G1 phase and cell apoptosis. The apoptosis regulates by various types of molecules such as Bcl-2 family protein, p53, and p21 (Fang et al., 2012). The molecules of Bcl-2 are expressed in different types of human cancers like liver, colon, and lung cancers and also in various types of solid tumours that stimulates the cell cycle (Fan et al., 2008).

The natural balsamin (type-1 RIPs) purified from *Momordica balsamina* has also shown anti-tumour activity in MCF7 and BT549 breast cancer cells *in-vitro* system (Ajjji et al., 2017). It is difficult to deliver protein-based drugs (antibodies, hormones and vaccines) in the GI tract (gastrointestinal tract) due to some conditions. The concentration of pH in human stomach is very low and the proteinases are present in very high amount, so the delivered protein degrades in the GI tract (gastrointestinal tract). To overcome this problem, studies have shown that nanoparticles have capability to protect the encapsulated macromolecules from the degradation process during the delivery in GI tract (gastrointestinal tract) (Bakhshi et al., 2017).

**Table 2.1:** Overview of different types of RIPs with antitumor activity

Type-1 RIPs	Source	Types of tumour	Study model	References

MAP 30	<i>Momordica charantia</i>	Brain glioblastoma, breast carcinoma, liver hematoma, myeloma neuroblastoma	<i>In-vitro</i>	(Lee-Huang et al., 1995)
MCP 30	<i>Momordica charantia</i>	Prostate cancer	<i>In-vitro</i>	(Xiong et al., 2009)
Alpha-MMC	<i>Momordica charantia</i>	Lung, liver, breast and epidermal cancer	<i>In-vitro</i>	(Bian et al., 2010)
Pokeweed	<i>Phytolacca americana</i>	T-cell leukaemia virus	<i>In-vitro</i>	(Mansouri et al., 2009)
TCS	<i>Trichosanthes kirilowii</i>	Hepatocellular carcinoma	<i>In-vitro</i>	(Fan et al., 2009)
Balsamin	<i>Momordica balsamina</i>	Breast cancer	<i>In-vitro</i>	(Ajji et al., 2017)
Type-2 RIPs				
Mistletoe	<i>Viscum album</i>	Ovarian, breast cancer	<i>In-vitro, in-vivo (humans)</i>	(Das et al., 2011)

### 2.3.2 Antiviral activities of RIPs

Ribosome-inactivating proteins play an important role in anti-plant virus activity. There are various RIPs are bound to sub-cellular parts: For example; apoplast or vacuoles for their synthesis. In some plants rRNA is very sensitive in depurination process through autologous (Mohanraj et al., 2010). To separate these enzymes from ribosome has a unique strategy to avoid their toxicity. During the depurination of rRNA cellular membrane disrupt then RIPs would be free from sub-cellular parts in the form of cytosol. In this mechanism localized cell would be dead and some limited pathogens spread (Zhang et al., 2016).

RIPs from *Momordica charantia* have broad-spectrum antiviral properties against different types of viruses through the inhibition of viral protein into the infected cells such as DNA and RNA viruses (Frederico et al., 2017). This ability of RIPs help to inactivate eukaryotic ribosome *in-vitro* for the mechanism of antiviral action that involves inactivation of host ribosome in virus-infected cells (Zeng et al., 2015).

Pokeweed antiviral protein (PAP) is most active antiviral protein to destroy the virus infections from plant species. PAP (pokeweed antiviral protein) from *phytolacca americana* also shows the antiviral activity (Table 2.2) towards the various viruses (Mansouri et al., 2009) as well as helps to inhibit the production of human T-cell Leukaemia (HTLV-1). HTLV-1 is delta retrovirus that acts as a causative agent of adult T-cell Leukaemia (Domashevskiy and Goss, 2015). PAP reduces the virus production by suppressing the expression of encoding gene HTLV-1 at the translational as well as transcriptional levels (Domashevskiy and Goss, 2015).

MAP30 RIPs inhibits the production of the hepatitis B virus (HBV). The introduction of HepG to MAP30 results in inhibition of HBV, DNA replication, and HBsAg secretion (Leung et al., 1987). MAP30 also inhibit the expression of HBV antigen so that DNA viral replication decreases and further reduces the synthesis of cDNA. The study shows that the high doses of MAP30 are effective in suppressing the viral replication by altering the kinetics of replicate DNA intermediates (Aji et al., 2017).

**Table 2.2:** Different types of RIPs with antiviral activities

Types of RIPs	Source (Scientific name)	Source (Tissue)	Types of viruses	
Alpha-momocharin	<i>Momordica charantia</i>	Seeds	Chilli veinal mottle virus, cucumber mosaic virus, tobacco mosaic virus	(Zhu et al., 2013)
PAP	<i>Phytolacca Americana</i>	Leaves	Tobacco mosaic virus	(Irvin, 1983)
New single-chain RIPs	<i>Basella rubra</i>	Seeds	Artichoke mottled crinkle virus	(Bolognesi et al., 1997)
CAP-34	<i>Clerrodendrum aculeatum</i>	Leaves	Papaya ringspot virus	(Srivastava et al., 2009)
CIP-29	<i>Clerdndum inerme</i>	Leaves	Tobacco mosaic virus	(Olivieri et al., 1996)
BDP-30	<i>Borhavia diffusa</i>	Roots	Tobacco mosaic virus	(Srivastava et al., 2015)
ME-1	<i>Mirabilis expansa</i>	Roots	Tobacco mosaic virus, Brome mosaic virus	(Vepachedu et al., 2003)
PAP I	<i>Phytolacca Americana</i>	Leaves	Zucchini	(Gu et al., 2017)
Trichosanthin	<i>Nicotiana tabacum</i>		Turnip mosaic virus, Cucumber mosaic virus, tobacco mosaic virus	(Lam et al., 1996)

### 2.3.3 Antifungal activity of RIPs

Ribosome-inactivating proteins have antifungal activity due to their *N*-glycosidase activity on rRNA. Some studies depicts that RIPs have the ability to protect the plants from different types of fungal infection (Citores et al., 2016). All of the fungi do not cause disease in plants however; some are beneficial for the plants.

It has been reported that RIPs are useful for the protection of plants from viral and fungal infections (transgenic tobacco) and it is used to test the fungal pathogens (Lam and Ng, 2001) . RIPs isolated from barley used in transgenic tobacco to demonstrate the robust activity against *R. Solani* (Table 2.3) infection during the plantation in contaminated soil (Logemann et al., 1992). All genes were under the control of an inducible promoter. Towards the next study, the tested fungi were check on many *in-vivo* and *in-vitro* to see the action of RIPs on tested pathogenic fungi (Mohanraj et al., 2010).

**Table 2.3:** overview of different types of RIPs with antifungal activity

Types of RIPs	Name of RIPs	Sources	Types of fungi	Reference
Barley RIPs	<i>Hordeum vulgare</i>	Seeds	<i>Trichoderma reesei</i>	(Roberts and Stewart, 1979)
ME1	<i>Mirabilis expansa</i>	Roots	<i>Pythium irregular, Fusarium oxysporum, Fusarium solani</i>	(Vivanco et al., 1999)
ME2	<i>Mirabilis expansa</i>	Roots	<i>Pythium irregular, Fusarium oxysporum, Fusarium solani</i>	(Vivanco et al., 1999)
Tobacco RIPs (TRIP)	<i>Nicotiana tabacum</i>	Leaves	<i>Trichoderma reesei, Cytospora canker, Fusarium oxysporum, Cochilobolus heterostrophus</i>	(Sharma et al., 2004a)
Alpha-momorcharin	<i>Momordica charantia</i>	Seeds	<i>Bipolaris maydis, Fusarium graminearum, Aspergillus oryzae, Aspergillus niger</i>	(Zhu et al., 2013)
MbRIP-1	<i>Momordica balsamina</i>	seeds	<i>Aspergillus niger, Sclerotinia sclerotiorum</i>	(Kushwaha et al., 2012b)
Luffacylin	<i>Luffa cylindrica</i>	Seeds	<i>Fuarium oxysporum, Mycosphaerella arachidicola</i>	(Parkash et al., 2002)
Hispin	<i>Benincasa hispida</i> var. <i>chieh-qua</i>	Seeds	<i>Copinus comatus, Fusarium oxysporum, Physalospora piricola, Mycosphaerella arachiicola</i>	(Wong et al., 2010)
Diocin 2	<i>Phytolacca dioica</i>	Leaves	<i>Pnicillium digitatum</i>	(Iglesias et al., 2005)
C. moschate RIP	<i>Cucurbita moschata</i>	Sarcocarp	<i>Phytophthora infestans</i>	(Barbieri et al., 2006)

#### 2.3.4 Antimicrobial activity of RIPs

RIPs are considered as a protein defence agents. Alpha-momorcharin from *Momordica charantia* has shown some results to interfere the growth of various fungal as well as bacterial pathogens (Table 2.4) such as *Fusarium*, *oxyporum*, *E.coli*, *P. aeruginosa*, *S. aureus*, *Fusarium solani* and *Bacillus subtilis* (Wang et al., 2012b).

**Table 2.4:** overview of different types of RIPs with antimicrobial activity

Types of RIPs	Name of RIPs	Sources	Types of bacteria	References
ME1	<i>Mirabilis expansa</i>	Roots	<i>Pseudomonas syringae</i> , <i>Agrobacterium tumefaciens</i> , <i>Agrobacterium radiobacetr</i>	(Vivanco et al., 1999)
ME2	<i>Mirabilis expansa</i>	Roots	<i>Pseudomonas syringae</i> , <i>Agrobacterium tumefaciens</i> , <i>Agrobacterium radiobacetr</i>	(Vivanco et al., 1999)
Tobacco RIPs (TRIP)	<i>Nicotiana tabacum</i>	Leaves	<i>Pseudomonas solanacearum</i> , <i>Erwinia amylovora</i> , <i>Shigella asonei</i> , <i>Salmonella typhimurium</i> , <i>Rhizobium leguminosarum</i>	(Sharma et al., 2004a)
Alpha-momorcharin	<i>Momordica charantia</i>	Seeds	<i>Pseudomonas aeruginosa</i>	(Wang et al., 2012a)
MbRIP-1	<i>Momordica balsamin</i>	Seeds	<i>Escherichia coli</i>	(Kushwaha et al., 2012b)
M. jalapa	<i>Mirabilis jalapa</i>	Leaves	<i>Propionibacterum acnes</i> , <i>Staphylococcu epidermidis</i>	(Zhu et al., 2018)
Balsamin	<i>Momordica balsamina</i>	Seeds	<i>Staphylococcus aureus</i> , <i>Salmonella enterica</i> , <i>Staphylococcus epidermidis</i> , <i>Escherichia coli</i>	(Aji et al., 2016)

### 2.3.5 Insecticidal activity of RIPs

Some types of RIPs showed the toxicity towards insects however, only few studies have been published which shows the effect of RIPs on insects (Ali et al., 2016). Type-1 RIPs such as saporin, geonin, momordin and PAP-S showed the endotoxic activity in various types of lepidopteran pests. These pests were used for soybean caterpillar *Anticarsia gemmatalis* and fall armyworm *Spodoptera frugiperda*. The micro-organism of RIPs affects the growth and development of *A. gemmatalis* and *S. frugiperda* during ingestion process. These both insects are sensitive to the type-1 RIPs (Stirpe et al., 1992).

According to record of US Department of Agriculture, there are almost one-tenth over 1 million insect species which are pests (Pizzo et al., 2015). From the study by Kumar and his co-worker, *Eranthis hyemalis* is a type-2 ribosome-inactivating protein, has antiviral activity, larvicidal activity against the alfalfa mosaic virus and the southern corn rootworm respectively (Kumar et al., 1993). The extracted seeds and leaves of plants were used as deterrent agent against pests of stored products as shown in Table 2.5.

**Table 2.5:** Insecticidal activity of different types of RIPs

Types of RIPs	Scientific name	Sources	Against insects	Reference
Ricin	<i>Ricin communis</i>	Seeds	Callosobruchus maculatus, Abies grandis, Bombyx mori	(A.M.R. et al., 1990)
Saporin	<i>Saponaria officinalis</i>	Seeds	Anticarsia gemmatalis, Spodoptera frugiperda	(Bertholdo-Vargas et al., 2009)
Lychnin	<i>Lychnis chalconica</i>	Seeds	Anticarsia gemmatalis, Spodoptera frugiperda	(Bertholdo-Vargas et al., 2009)
Momordin	<i>Momordica charantia</i>	Seeds	Anticarsia gemmatalis, Spodoptera frugiperda	(Bertholdo-Vargas et al., 2009)
PAP-S	<i>Phytolacca Americana</i>	Leaves	Anticarsia gemmatalis, Spodoptera frugiperda	(Bertholdo-Vargas et al., 2009)
Cinnamomin	<i>Cinnamomum camphora</i>	Seeds	Helicoverpa zea, lasioderma serricone	(Zoubenko et al., 2000)
Gelonin	<i>Gelonium multiflorum</i>	Seeds	Anticarsia gemmatalis, Spodoptera frugiperda	(Bertholdo-Vargas et al., 2009)
Type-1 RIPs	<i>Malus domestica</i>	Leaves	Acrythosiphon pisum, Myzus persicae, Spodoptera exigua	(Hamshou et al., 2017)
Type-2 RIPs	<i>Malus domestica</i>	Leaves	Acrythosiphon pisum, Myzus persicae, Spodoptera exigua	(Hamshou et al., 2017)

## 2.4 STRUCTURE FUNCTIONS OF TYPE-1 RIPs

### 2.4.1 The structure of Ricin

The first three dimensional structure of of RIPs (Ricin) from *Ricin communis* was obtained through crystallography and refined to 1.8Å resolution. The overall structure of Ricin was in ribbon shape, approximately 50% of the polypeptide divided into  $\alpha$ -helix or  $\beta$ -sheet (Yamini et al., 2015). The Ricin chain has heterodimer structure and the monomer units were joined by a single disulphide bond. The Ricin chain consists of 267 globular proteins, which is the active site to recognize the rRNA stem-loop (target). The B chain of Ricin consists of 263 residue of amino acids and it also consists of galactose binding site (Nicolas et al., 1997). From the experimental data the Ramachandran outlier's value of this protein is 0 and side chain value is 8.8%. It is classified as hydrolase with X-Ray diffraction method as shown in Figure 2.2.

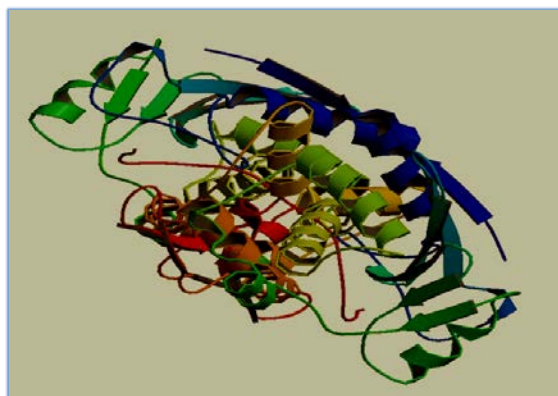


**Figure 2.2:** The ribbon diagram of Ricin (1 IFT) that has been reproduced from Protein Data Bank ([www.pdb.org](http://www.pdb.org)). Alpha-helix is shown in red colour and loop region is shown in blue colour in the given figure

### 2.4.2 The ribbon structure of MAP30

The basic structure of MAP30 from *Momordica charantia* was deduced by NMR spectroscopy. MAP30 is type-1 ribosome-inactivating protein with molecular weight 30 kDa. It has 263 amino acid .The N-terminal domain consists of residue from 1 to 105. It consists of six mixed  $\beta$ -sheets which are packed against  $\alpha$ -helix. This forms a central domain consisting residues from 108 to 180 (Wang et al., 1999). The C-terminal domain (residues 181-263) contains anti-parallel  $\beta$ -sheets packed against long bent helix (residue 181 to 200).

The various residue present in C-terminal domain (Try-70, Try-109, Glu-158 and Arg-161 are associated with RNA and glycosidase activity (Mak et al., 2007). The location of RNA and glycosidase pocket is in the centre of the groove of the protein (Figure 2.3).

The negatively charged residues which are located on the surface of the groove to the right side of RNA and glycosidase pocket are Glu-110, Glu-121 AND Glu-187. The residues present to the left of the RNA and glycosidase pocket are Asp-43, Asp-65, Glu-85 and Glu-89. The Ramachandran outlier is 6.9% and side chain outliers are 14.3%.

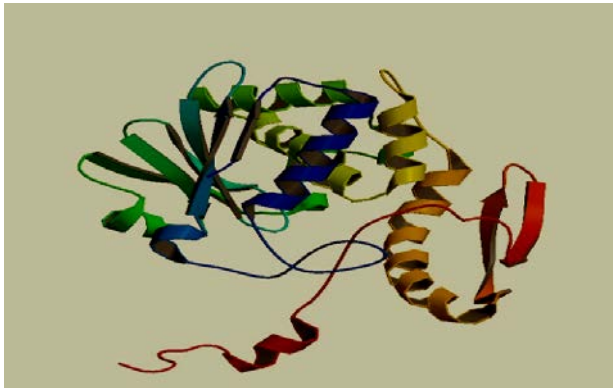


**Figure 2.3:** The ribbon structure of MAP30 (1D8V) that has been reproduced from [www.pdb.org](http://www.pdb.org) (Protein Data Bank). A-helix is shown in red colour and loop region is shown in green colour in the given figure.

# **Chapter 3:**

## **Material and methods:**

## **The objective and hypothesis of the research project:**

1. Isolation and partial purification of RIPs (Balsamin protein): The first objective of the research project was partial purification of balsamin from the seeds of *Momordica balsamina* and evaluate the beneficial activities of the protein.
2. Bioinformatics Analysis: The second objective of the research project was to find the phylogenetic similarities between the different types of ribosome-inactivating proteins from same plant genera.
3. Biological activity of balsamin: The third objective of this study was to find the DNase-like activity of balsamin.

## **Hypothesis:**

The hypothesis to be tested in this project is that balsamin i.e. type-1 ribosome-inactivating proteins will show DNase-like activity.

### 3.1 Diagrammatic representations of the purification process

Seeds of *Momordica balsamina*



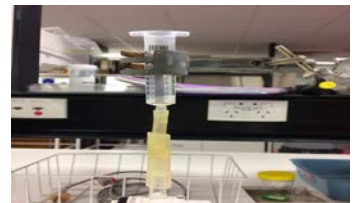
Ammonium sulphate precipitation



Protein sample in Dialyzed membrane



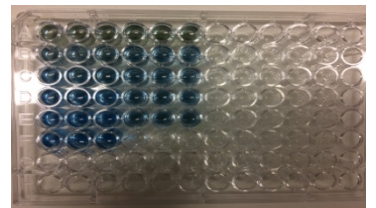
Ion-exchange Column Chromatography (with CM-Sepharose)



SDS-PAGE gel electrophoresis



Protein Estimation with Bradford assay



Functional Analysis: Biological Activity and Bioinformatics analysis

Figure 3.1: The schematic presentation of protein purification.

## 3.2 MATERIAL AND METHODS

To fulfil the objectives of this study following materials and methods were followed. The outline of the research project is presented in Figure 3.1. CM-Sepharose (CAS#68894-07-05) and other chemicals including sodium chloride, monobasic sodium phosphate, dibasic sodium phosphate, hydrochloric acid, dialysis membrane, and ammonium sulphate were obtained from Sigma-Aldrich. All the chemicals used in this project were of analytical grade obtained from sigma or Bio-Rad.

### 3.3.1 EXTRACTION OF BALSAMIN FROM THE SEEDS OF *MOMORDICA BALSAMINA*

The seeds of *Momordica balsamina* were provided in the laboratory. 20 g seeds of *Momordica balsamina* were decorticated then ground by mortar and pestle to make in the powder form. The powder form of seeds was homogenized in 50 mL of 150 mM NaCl. To make 500 ml of NaCl buffer, add 4.383 g (w/v) of NaCl and dissolve in MilliQ water. The mixture of sample was stirred speed at 4 °C then the slurry was filtered through muslin cloth. The crude sample of balsamin after filtration centrifuged at  $10,000 \times g$  for 20 min at 4 °C (Beckman Coulter Allegra™ X-12R Centrifuge, U.S.A). After centrifugation the clear supernatant was collected then precipitated the protein sample with solid ammonium sulphate (0-60%) while constant stirring using a magnetic stirrer at 4 °C according to the method described by (Kaur et al., 2012).

### 3.3.2 AMMONIUM SULPHATE PRECIPITATION AND DIALYSIS OF BALSAMIN

Ammonium sulphate was used for the precipitation of protein. Phosphate buffer was made with monobasic sodium phosphate and dibasic sodium phosphate both chemicals were obtained from Sigma-Aldrich. The 1 L volume of buffer was made with 1.56 g (w/v) of monobasic sodium and 1.41 g (w/v) dibasic sodium then adjusts the pH of buffer solution at 6.5 with sodium hydroxide or hydrochloric acid. The solid ammonium sulphate was added very slowly and kept the solution for 8 hours to complete the precipitation process. After precipitation, the crude sample of balsamin

was centrifuged (Beckman Coulter Allegra™ X-12R Centrifuge, U.S.A) at  $10,000 \times g$  for 10 minutes at 4 °C. The supernatant was discarded and pellet re-suspended in 15 ml (w/v) of 10 mM phosphate buffer, pH 6.5 (Buffer A). The precipitation solution was dialyzed in the dialysis membrane (from Sigma-Aldrich) for overnight in the presence of buffer A (phosphate buffer at pH 6.5) in a 500ml beaker at 4 °C (Adriano, 1989). The protein solution was then transferred to clean and fresh tube and pooled the solution at temperature 4 °C for further purification of protein.

### **3.3.3 THE ESTIMATION OF PROTEIN**

Bradford assay was performed to determine the estimation of protein concentration a (Bradford, 1976). Bradford dye consists of 5mg (w/v) Coomassie brilliant blue dye G-250, 5mL (v/v) Methanol and 10mL (v/v) of 85% Phosphoric acid then volume up the solution with MilliQ water and filtered through Whatman filter paper (Grade 1, 75 mm). Bovine serum albumin was used as the protein standard of 1 (w/v) mg/mL to 0.03125 (w/v) mg/mL concentrations were diluted and used to make the standard curve. A 96 well-plate was used to make standard curve, 10  $\mu$ L of standard and protein sample were loaded on the appropriate wells with three replicates and 200  $\mu$ L of diluted dye poured to the each well and mix properly. The sample was incubated at room temperature for 15-30 min to allow protein to bind with a dye. The absorbance of the sample was measured at 595 nm on FLUOstar™ plate reader (BMG Labtech, Germany).

### **3.3.5 ION-EXCHANGE CHROMATOGRAPHY**

CM-Sepharose column slurry (GE Health science, USA) was used for ion-exchange chromatography. To purify 20 g sample of balsamin (possessing protein concentration 1.468 mg/ml) 1 mL slurry was used for ion-exchange chromatography. For preparing a CM-Sepharose column, a 10 mL disposable syringe was used. The ion-exchanger (CM-Sepharose) is equilibrated to the working temperature before being packed, the column then degasses the CM-Sepharose. To degas the gel, gel was suspended in 2-4 fold excess of buffer then allowed 95% of the gel to settle down, aspirate off the remaining gel by vacuum suction. The slurry was placed in thick-walled Erlenmeyer flasks with a side-arm. The top of the flask was sealed with rubber stopper then the vacuum tubing was attached with the sidearm of the Erlenmeyer flasks. The flask should be swirled

every 15 min till the bubbles were no longer appeared in the slurry. The 1 L slurry (CM-Sepharose) poured in the column and was left overnight to settle the gel. Firstly, column was equilibrated with five volumes of buffer A (10 mM phosphate buffer) consisted of monobasic sodium phosphate and dibasic sodium phosphate at pH 6.5) then the protein sample was loaded into the column. The fractions which had contained proteins were eluted from the column using linear gradient of 0-0.4 NaCl buffer in 10 mM phosphate buffer at pH 6.5 (buffer B). The fractions which had the higher peak of absorbance were pooled then identified using UV-Spectrophotometer (T70 UV-Spectrophotometer) at absorbance of 280 nm. Most of the protein was retained on the CM-Sepharose column which means that the collected proteins are basic in nature.

### **3.3.6 SDS-PAGE GEL ELECTROPHORESIS**

The polyacrylamide gel electrophoresis procedure was performed according to method described by (Laemmli, 1970). The samples of protein were diluted in 1:3 sample buffer in 1× running buffer containing 5ml of 50mM Tris HCL at pH 6.8, 4ml Glycerol, 0.8 g SDS, 2 µL OF Saturated bromophenol blue and 0.62 g (0.062g/ml) DDT (Dichlorodiphenyltrichloroethane) added freshly before used the sample loading buffer. The 12% acrylamide resolving gel consisted of 1250 µl of 1.5M Tris HCL at pH 8.8, 50 µl of 10% SDS (0.1 g/ml), 1660µl of MilliQ water, 2082 µl of 30% acrylamide, 50 µl of 10% Ammonium sulphate (APS) and in the last add 5 µl TEMED (Tetramethylethylenediamine) (Table 3.1). Following concentration of solution was used to prepare 4% stacking gel, 1000 µL of 0.5 M HCL at pH 6.8, 50 µl of 10% SDS, 2298 µL MilliQ water, 670 µL of 30% Acrylamide and 5 µL of TEMED (Table 3.2). Acrylamide stacking gel was stained with Coomassie brilliant blue-G for 30 min. Coomassie staining solution was consisted of 40% (v/v) Methanol, 10% acetic (v/v) acid and 0.1% (w/v) Brilliant Blue R-250 (Merck, USA) on racking platform. SDS-PAGE gel then de-stained with Coomassie de-staining solution which consists of 20% (v/v) Methanol, 10% (v/v) acetic acid and make up the volume 1 L by adding Milli Q water. The bands of protein were visualized using Gel Doc™ SYSTEM and Imager Lab™ (Bio-Rad, USA).BIO-RAD electrophoresis chamber and casting frame was used to run and make the gel respectively.

### 3.3.7 CONCENTRATION OF PROTEINS

The fractions that contained low-molecular weight proteins (as evidence from the SDS-PAGE gel) were pooled then these fractions were concentrated by ultrafiltration membrane (Amicon ultra-15 10 kDa, US) for further purification of protein. The concentrated fractions were treated with plasmid to investigate the DNase-like activity. To determine the concentration of protein, Bradford assay was used. BSA (bovine serum albumin) was used as a standard to make the standard curve. The concentration of protein in unknown samples was calculated from standard curve. Concentration of balsamin using Ammonium sulphate precipitation as shown in Table 3.3.

**Table 3.3:** The concentration of protein found in the samples using Ammonium sulphate precipitation

Fraction of protein	Concentration of protein (mg/ml)
Crude sample	1.438
20% Ammonium sulphate precipitation	0.0282
40% Ammonium sulphate precipitation	0.832
60% (after 40%) Ammonium sulphate precipitation	0.949
60% Ammonium sulphate precipitation	1.225

### 3.3.8 DNase LIKE ACTIVITY OF BALSAMIN

The concentrated protein was treated with plasmid to investigate DNase-like activity. To determine DNase-like activity of balsamin. PEGFP plasmid was used as a substrate. NanoDrop™ obtained from Thermo Fisher™ was used to determine the concentration of plasmid. Various concentrations of balsamin from ion-exchange chromatography (0.5-2 µg of balsamin) were

incubated with 0.25 µg PEGFP plasmid DNA in a final volume of 10 µL of assay buffer consists 50 mM Tris HCL at pH 7.5, 50 mM KCL, 0.1 mM MgCl<sub>2</sub>. The reaction mixture was incubated at 37 °C for 2h. Digestion of the plasmid with restriction endonuclease EcoRI served as a positive control. The reaction of DNA is extracted using Qiagen PCR purification kit then analysed on 0.8% agarose gel. Agarose gel was prepare: 0.32 g (w/v) agarose powder was dissolved in 40 ml of 50x TBE buffer as described by (Puri et al., 2009)

### **3.3.9 AMINO ACID SEQUENCE AND BIOINFORMATICS ANALYSIS OF BALSAMIN**

The sequence alignment of balsamin (the sequence was retrieved from NCBI, <https://blast.ncbi.nlm.nih.gov/Blast.cgi> with Accession number: 3V2K\_A) was performed with BLAST program. The different types of ribosome-inactivating proteins were sequenced with BLAST such as alpha-momorcharin from *Momordica charantia* (gi: 60459323), b-luffin from *Luffa aegyptiaca* (gi: 19150), bryodin from *Bryodin dioica* (gi: 2981957), trichosanthin from *Trichosanthes kirilowii* (gi: 547149), trichomislin from *Trichosanthes kirilowii* (gi: 46403107), trichobakin from *Trichosanthes species* (gi: 7242890), Lychnin from *Silene chalcedonica* (gi: 44434) and found the closely related spices of balsamin (Bandehpour et al., 2017). All the sequence was saved in FASTA format and then the alignments of all sequence was conducted using Clustal X<sub>2</sub> software (<http://www.clustal.org/download/current/>). All aligned sequence file was saved in .aln file and convert this .aln file into .meg file with MEGA6 software (<https://www.megasoftware.net/>). This software was used to make phylogenetic tree (Jones et al., 1992). Phylogenetic tree was made based on the basis of genetic information of protein.

### **3.3.10 BUILDING THE PROTEIN MODEL**

The model of balsamin was built with SWISS-MODEL. SWISS-MODEL is online server as (<https://swissmodel.expasy.org/> ). Alpha-MMC was used as a template to predict the model of balsamin. The 3D structure of alpha-MMC with the target sequence was built automatically.

### **3.3.11 ASSESSMENT OF MODEL WITH RAMACHANDRAN PLOT**

The generated model from SWISS-MODEL has to verify. To validate the 3D structure of alpha-MMC, Ramachandran plot was used. Ramachandran is an online tool available on online (<http://mordred.bioc.cam.ac.uk/~rapper/rampage.php> ).

# **Chapter 4:**

## **Result and Discussion:**

Ribosome-inactivating proteins (RIPs) are toxic N-glycosidase that inhibits the particular conserved loop of large rRNA. During this depurination the ribosome are inactive and its further participation in protein synthesis were blocked. In this study balsamin, a type-1 RIPs from the

seeds of *Momordica balsamina* has been purified and characterized its biochemical and biophysicochemical properties.

#### **4.1 MORPHOLOGICAL STUDIES**

*Momordica charantia* commonly known as bitter melon and bitter gourd in English is a fast growing vine that belongs to *Cucurbitaceae* family. It has received great attention since it produces ribosome-inactivating proteins that possess anticancer, antiviral, antifungal activities. Recently, researchers have been showing their interest to investigate the antifungal activities of *M. charantia* (Narsing Rao et al., 2017).

*Momordica balsamina* also possess type-1 RIPs which belongs to *Cucurbitaceae* family (Kaur et al., 2012, Puri et al., 2012, Aji et al., 2017). It is a high-climbing vine and the fruit of this plant is regular or irregular rows of short blunt spines. This plant is used to cure wounds, snake bite and skin rash (Bolognesi et al., 2016). It has pale yellow flower and the fruit of this plant is in green or yellowish short blunt spines which on ripening turn to bright orange or red as shown in Figure 4.1. The seeds of this plant are one quarter an inch long and the orange pulp contains seeds covered with a bright red skin.



**Figure 4.1: Different stages of *Momordica balsamina* plant showing (a) flower (b) fruit and (c) ripened fruit (This information has been reproduced from <https://www.google.com.au/search?q=momordica+balsamina&source> ).**

The seeds of *M. balsamina* were provide in the laboratory to purify balsamin based on an optimised protocol (Aji et al., 2016)

## **4.2 PURIFICATION OF Balsamin**

To purify the protein from the seeds of *Momordica balsamina* various biochemical techniques were used.

### **4.2.1 Ammonium sulphate precipitation**

The crude extract (prepared in NaCL buffer) of *M. balsamina* was filtered through muslin cloth then centrifuged. Ammonium sulphate precipitation of balsamin was did into three parts, in the first part the sample of balsamin was precipitated from 20% to 60%, in the second part the sample of protein was precipitated from 40% to 60% and in the third part of balsamin, it was precipitated with 60% of ammonium sulphate. Most of the protein was precipitated at 60% ammonium sulphate precipitation. The pellet obtained as result of centrifugation was re-suspended into 10 mM phosphate buffer pH 6.5 and then dialyzed in the presence of 10 mM phosphate buffer to remove

the excess amount of salts from the precipitated sample. The dialyzed sample of protein was used for further purification of protein.

The precipitated sample of protein was analysed with SDS-PAGE electrophoresis as shown in Figure 4.2.

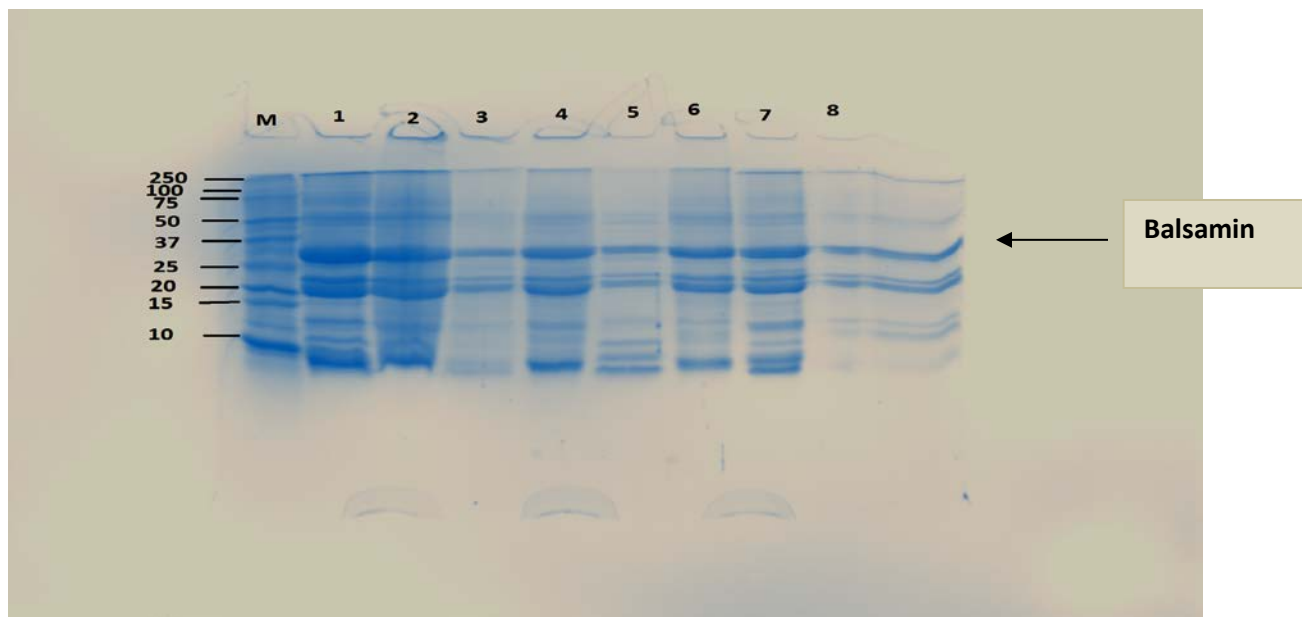


**Figure 4.2: SDS-PAGE analysis of Ammonium sulphate precipitation**

Lane M contains protein standard Myosin (250 kDa),  $\beta$ -Galactosidase (150 kDa), Bovine serum albumin (100 kDa), and Glutamine dehydrogenase (75 kDa), Ovalbumin (50 kDa), Carbonic anhydrase (37 kDa), Lysozyme (20 kDa) and Aprotinin (10 kDa). Lane 1: crude sample of protein, Lane 2: supernatant of protein, Lane 3: 20% ammonium precipitation. Lane 4: 40% (after 20%) ammonium precipitation, Lane 5: 60% (after 20% to 40%) ammonium precipitation, Lane 6: 40% ammonium precipitation, Lane 7: 60% ammonium precipitation, Lane 8-10: 60% ammonium precipitation.

#### 4.2.2 Ion-exchange chromatography

The dialyzed protein sample was subjected to ion-exchange chromatography. CM-Sepharose was used in the chromatography method. Firstly, the column was equilibrated with 10 mM phosphate

buffer at pH 6.5 (Buffer A). Most of the protein was retained on the CM-Sepharose column; however, un-bound proteins from column were eluted with buffer A (10 mM phosphate buffer at pH 6.5). Bound proteins were eluted with elution buffer of 0-0.4 mM NaCl. The elution at 0.1 mM NaCl resulted in highest peak; (BI Figure 4.3), followed by other minor peaks (BII-BIV). The fractions has higher absorbance value was run on SDS-PAGE gel electrophoresis to find the molecular weight of proteins (Figure 4.4).

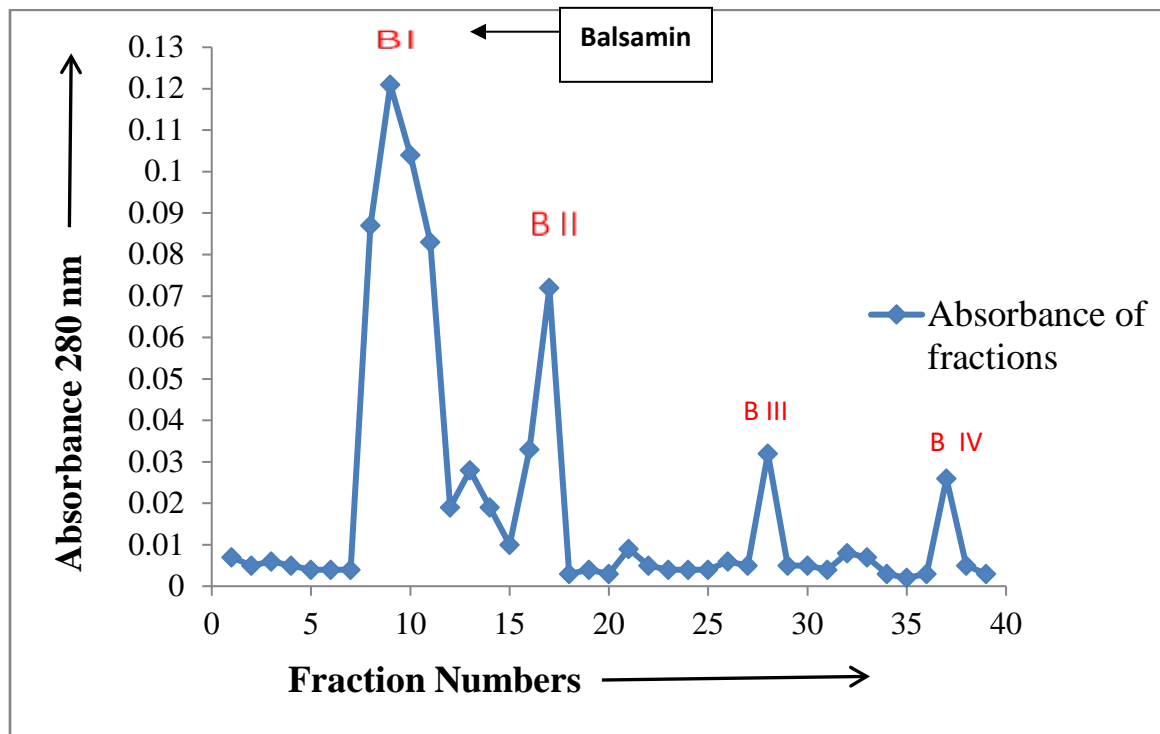


**Figure 4.3:** Profile of Ion-exchange chromatography of CM-Sepharose fractions. These fractions were eluted with a buffer possessing variable sodium chloride concentration (BI-BIV with 0.1 mM-0.4 mM NaCl) which has the highest peaks are pooled separately and represented as BI, BII, BIII, and BIV with different concentration of elution buffer.

#### 4.2.3 SDS-PAGE gel electrophoresis of ion-exchange chromatography fractions

SDS-PAGE gel electrophoresis was used to determine the molecular weight of protein. All eluted fractions from ion-exchange chromatography were run on SDS-PAGE gel to ascertain molecular weight of the proteins (Figure 4.4).

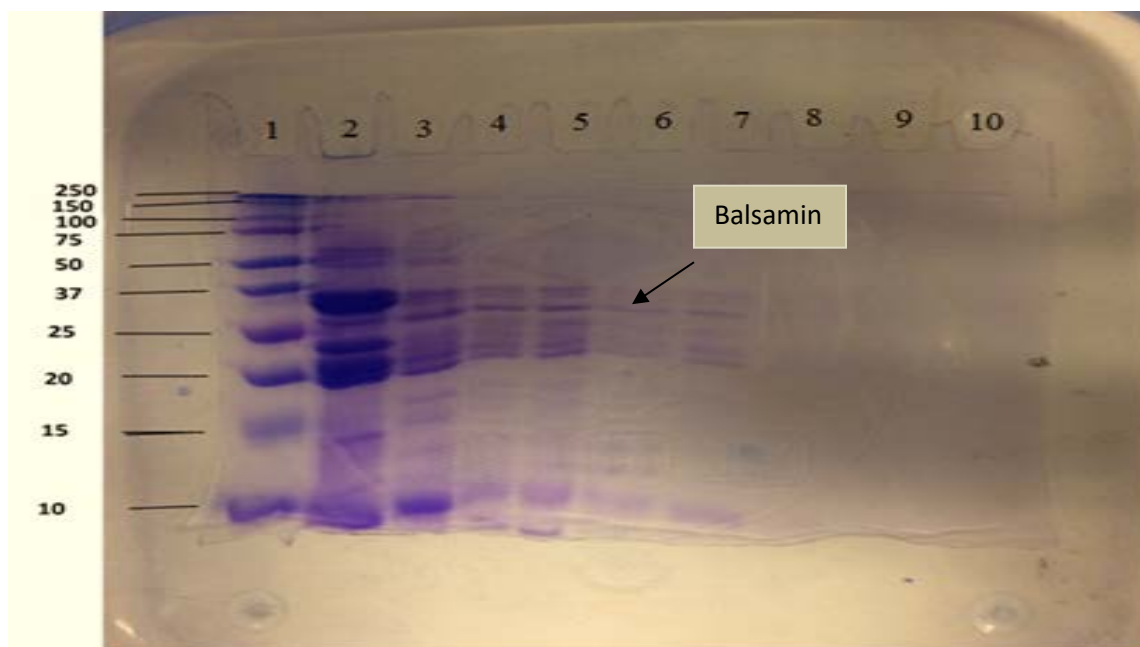


**Figure 4.4:** SDS-PAGE analysis of ion-exchange chromatography fractions.

**Lane 1 has protein standard (Precision Plus protein™ dual colour protein standard has used which contained Myosin (250 kDa),  $\beta$ -Galactosidase (150 kDa), Bovine serum albumin (100 kDa), Glutamine dehydrogenase (75 kDa), Ovalbumin (50 kDa), Carbonic anhydrase (37 kDa), Lysozyme (20 kDa) and Aprotinin (10 kDa) Lane 2: Crude sample of protein, Lane 3: Ammonium sulphate precipitation, Lane 4: 0.1 mM NaCl elution buffer, Lane 5: 0.2 mM NaCl elution buffer, Lane 6: 0.3 mM NaCl elution buffer, Lane 7: 0.4 mM NaCl elution buffer, Lane 8: Free NaCl elution buffer.**

The partially purified protein ( $\mu$ l or mg) as evidenced from SDS-PAGE gel (Lane 5 in Figure 4.4) was used for conducting biological activity. These fractions were concentrated by Amicon Ultra-15 filtration (10 kDa), and concentrated protein was kept in the refrigerator for conducting biological activity.

#### **4.2.4 DNase LIKE ACTIVITY OF BALSAMIN**

DNase like activity of the partially purified balsamin was investigated using different concentrations of balsamin (0.5  $\mu$ g) with plasmid (0.25  $\mu$ g) as described by (Puri et al., 2009). The

plasmid with balsamin caused changes in the conformation of DNA. As a result, first cleaved the DNA supercoiled forms into linear form of DNA. Treatment of balsamin with plasmid showed the conversion of supercoiled DNA into linear form as visualized on agarose gel electrophoresis. The low amount of balsamin did not shows any changes in DNA conformation and with the increased amount of balsamin, the open circular DNA band gradually appeared (Lane 3 in Figure 4.5).

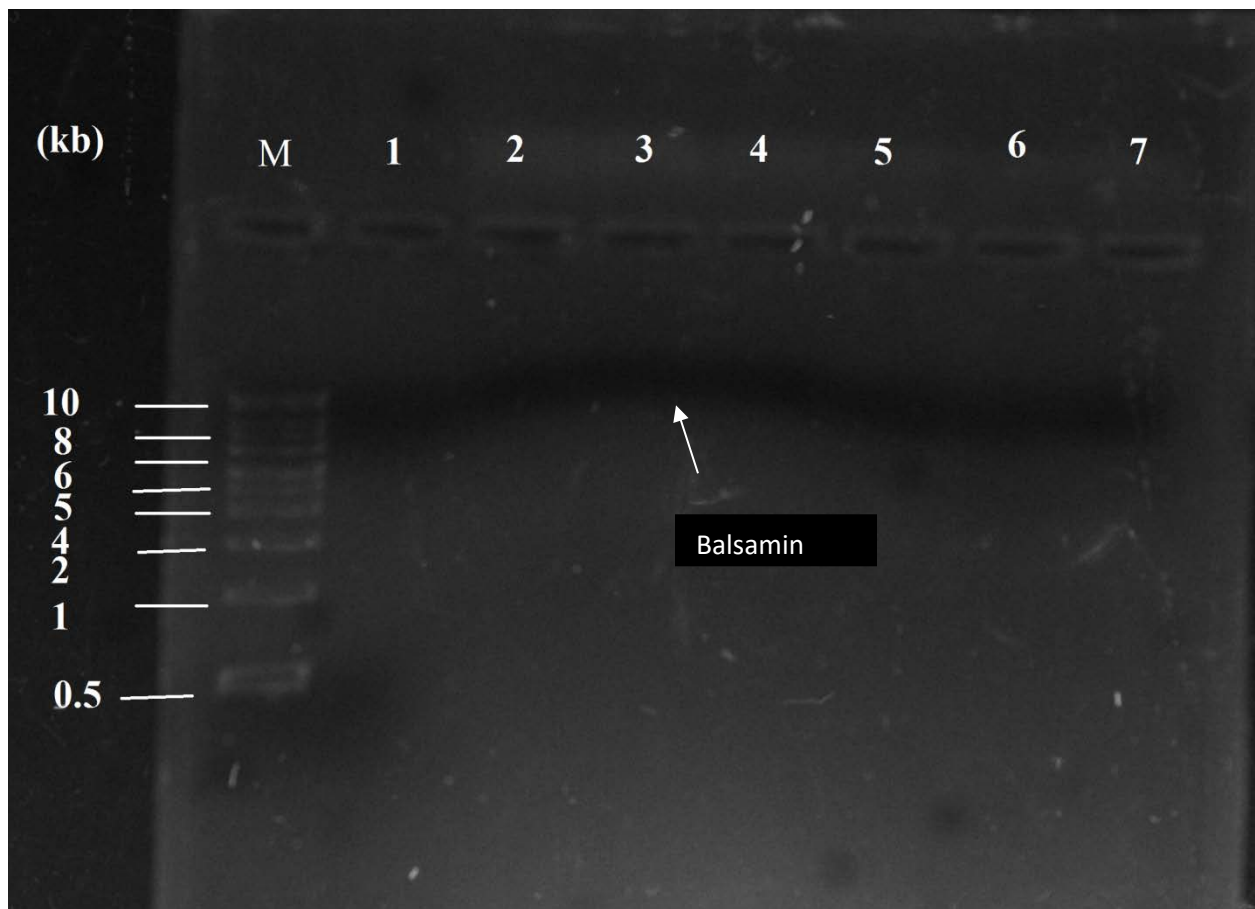


**Figure 4.5:** Agarose gel electrophoresis analysis of DNase-like activity of balsamin.

**Lane M:** 1 kb DNA ladder, **Lane 2** is 0.25 µg Plasmid, **Lane 3** is 0.5 µg balsamin with plasmid

**Lane 4 to lane 7:** 0.5 µg balsamin with plasmid (fractions from ion-exchange chromatography)

## 4.3 BIOINFORMATICS ANALYSIS

### 4.3.1 Prediction of biophysical and physiochemical parameters of a protein

To predict the biophysical and physiochemical parameters of protein the PROTPARAM expasy protein analysis online tool (<https://web.expasy.org/protparam/>) was used. The PROTPARAM program of the expasy is the online tool which helps to understand various biophysical and physiochemical parameters as shown in Table 4.1.

The analysis showed that balsamin consisted of 285 amino acids; with a predicted molecular weight 31.5 kDa and an isoelectric point is 9.13. The protein consisted of 24 positively and 28 negatively charged amino acids. Balsamin is a stable protein due to its instability index 29.33.

It is classified that protein is stable due its instability index (IT) which is 29.33 and the aliphatic index of this protein is 101.64 with 0.016 grand average of hydropathicity (GRAVY).

**Table 4.1:** The biophysical and physiochemical parameters of balsamin were predicted with PROTPARAM Expasy protein analysis tool.

<b>Biophysical and biochemical parameters</b>	<b>Predicted parameters</b>
<b>Molecular weight</b>	31.5
<b>Number of amino acids</b>	286
<b>Theoretical Pi</b>	9.13
<b>Total number of negative charged residues</b>	24
<b>Total number of positive charged residues</b>	28
<b>Total number of atoms</b>	4479
<b>Extinction coefficient</b>	26360
<b>Abs 0.1%</b>	0.8363
<b>Estimated half-life</b>	30 hours (mammalian reticulocytes, <i>in-vitro</i> ) >20 hours (yeast, <i>in-vivo</i> ) >10 hours (Escherichia coli, <i>in-vivo</i> )
<b>Instability index</b>	29.33
<b>Aliphatic index</b>	101.64
<b>GRAVY</b>	0.016

#### 4.3.2 Protein Identification with RIPs type-1

The sequences of amino acids of balsamin were used to check the homology relationship of balsamin with other type-1 RIPs with BLAST program. The amino acid sequences alignment of balsamin with other types of RIPs exhibited in Figure 4.6.

**Table 4.2** PDB BLAST analysis was performed with amino acid sequences of balsamin.

<b>Plant species</b>	<b>Name of protein</b>	<b>Accession number</b>	<b>Identity (%)</b>	<b>E-value</b>
<i>Momordica charantia</i>	<b>Alpha MMC</b>	<b>AAB22586</b>	<b>93</b>	<b>7e-06</b>
<i>Luffa aegyptica</i>	<b>Luffin-b</b>	<b>CAA44230.1</b>	<b>54</b>	<b>0.004</b>
<i>Bryodin dioica</i>	<b>Bryodin</b>	<b>1BRY_Y</b>	<b>68</b>	<b>0.045</b>
<i>Trichosanthes kirilowii</i>	<b>Trichosanthin</b>	<b>2019502A</b>	<b>74</b>	<b>0.76</b>
<i>Trichosanthes kirilowii</i>	<b>Trichosamislin</b>	<b>AAS92579</b>	<b>74</b>	<b>0.48</b>
<i>Trichosanthes kirilowii</i>	<b>Trichobakin</b>	<b>BAA92530</b>	<b>70</b>	<b>0.48</b>

The E-value predicates the relationship of the sequence of similar score. The alignments are more significant which has the smaller E-value.

The amino acid sequences (Table 4.3) from different types of RIPs from different plants were taken to find their phylogenetic relationship. The phylogenetic tree shows that balsamin has close relationship with  $\alpha$ -MMC and from the result it shows that other RIPs like Trichomislin from *T.kirilowii* are more close to bryodin from *Bryonia dioica* than balsamin (Table 4.2).

To show the evolutionary relationship of ribosome-inactivating proteins different types of plants were used in the phylogenetic tree. The phylogenetic tree depicts that balsamin is more similar with  $\alpha$ -MMC because they both are on the same branch and the other types of ribosome-inactivating proteins are originated from this branch in phylogenetic tree (Figure 4.7).

## 4.4 Sequence alignment

Sequence alignment is used to align the target protein primary amino acid sequence with template protein amino acid sequence to find the structurally and functionally conserved region. The alignment of all proteins were done with bioinformatics programs such as Clustal X2 and MEGA6 to consider the secondary structure of balsamin and determine the relationship with other protein from phylogenetic tree respectively.

### 4.4.1 Sequence alignment of protein

Alpha-momorcharin (1F8Q) used as template for the sequence alignment because it was identified more similar (98.8%) with balsamin. Also the crystal structure of this protein is available online. Protein sequence alignment was done with BLAST. The sequence alignment of  $\alpha$ -MMC is shown in Figure 4.6.

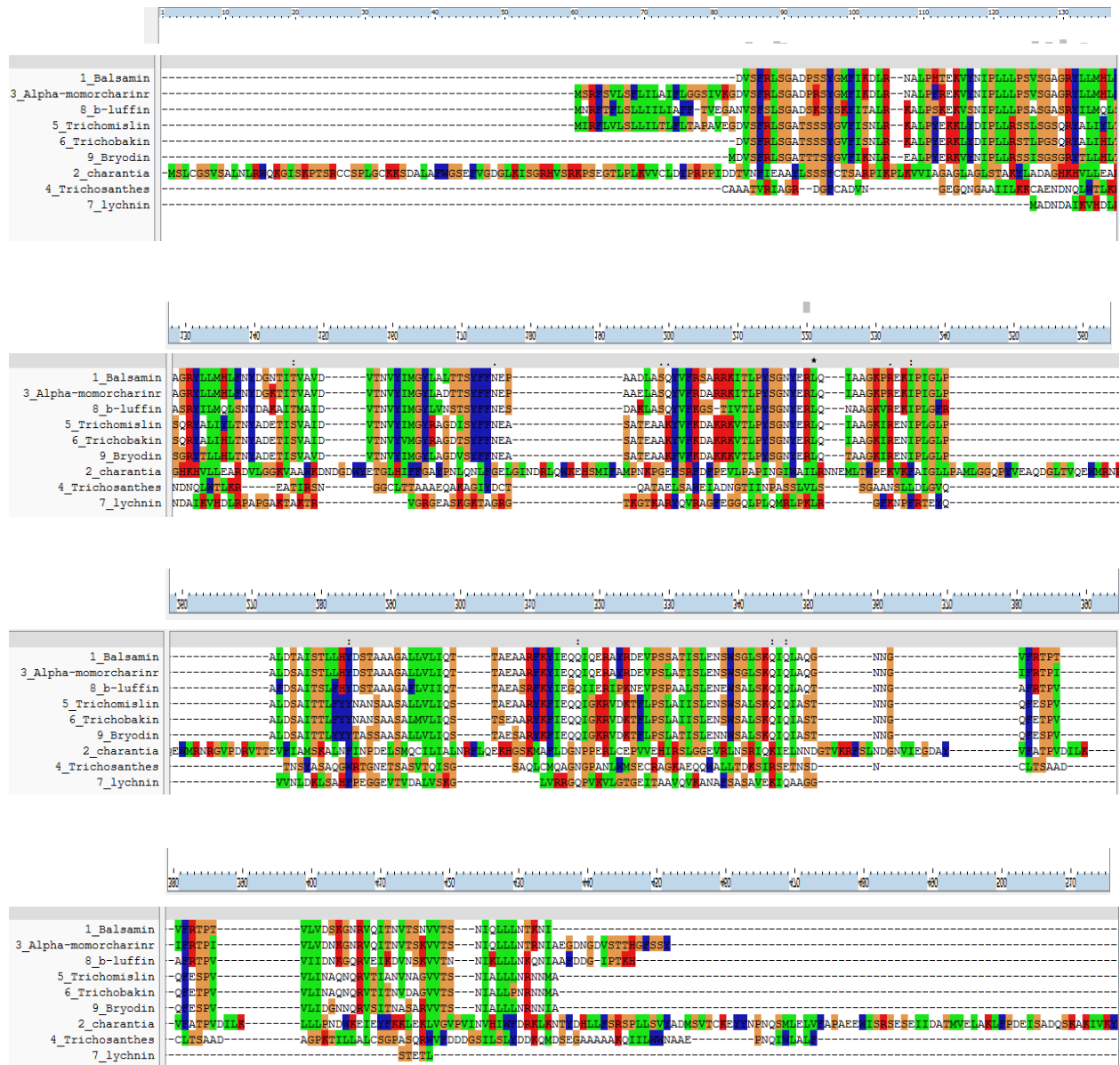


**Figure 4.6:** The amino acid sequence alignment of balsamin with other types of ribosome-inactivating protein from plants such as: alpha-momorcharin from *Momordica charantia* (gi: 60459323), b-luffin from *Luffa aegyptiaca* (gi: 19150), bryodin from *Bryodin dioica* (gi: 2981957), trichosanthin from *Trichosanthos kirilowii* (gi: 547149), trichomislin from *Trichosanthos kirilowii* (gi: 46403107), trichobakin from *Trichosanthos species* (gi: 7242890), Lychnin from *Silene chalcedonica* (gi: 44434).

## 4.5. Phylogenetic tree of balsamina

Phylogenetic tree is a branching diagram which is used to depict the evolutionary relationship among different organisms. To make phylogenetic tree of balsamin and shown their relationship with other types of RIPs, various types of type-1 RIPs are used from different kind of plants. From the phylogenetic tree of balsamin, it shows that *Momordica balsamina* has a close relationship with  $\alpha$ -MMC because they both are on the same branch, however *Momordica balsamina* has much different from Lychnin. The phylogenetic relationship with all type-1 RIPs as shown in Figure 4.5.1

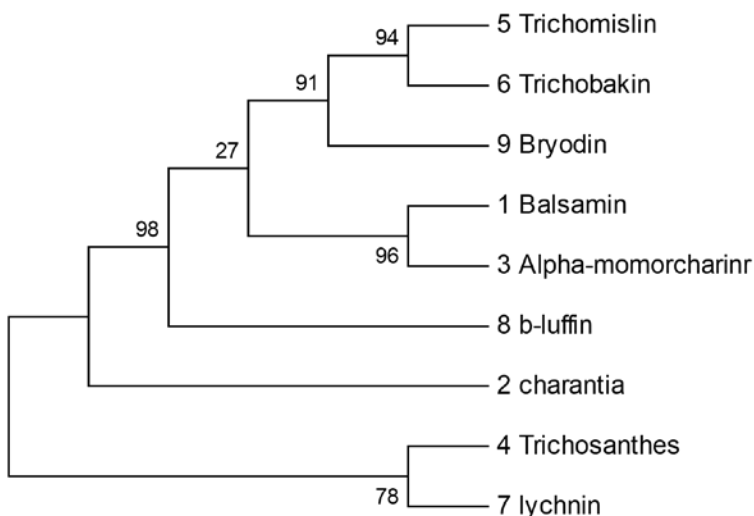


**Figure 4.7.** Molecular Phylogenetic analysis by Maximum Likelihood method (<https://www.megasoftware.net/>.)

The evolutionary history is inferred by using the Maximum Likelihood method based on the JTT matrix-based model. The percentage of trees in which the associated taxa clustered together is shown next to the branches (Jones et al., 1992). The analysis involved 8 amino acid sequences. All positions containing gaps and missing data are eliminated. There are a total of 219 positions in the final dataset. Evolutionary analyses are conducted in MEGA6 (Tamura et al., 2013).

## 4.6 BUILDING THREE DIMENSIONAL MODEL OF ALPHA-MMC

The sequence of protein has been aligned with the target sequence of protein to build a model of a protein. The aligned sequence from Clustal X2 was submitted to SWISS-MODEL to build a model (Table 4.4). The three dimensional  $\alpha$ -MMC structures were built automatically with SWISS-MODEL.

SWISS-MODEL online tool was used to predict the structure of protein (TABLE 4.5). Alpha-MMC was used as template in this server (Figure 4.8) and the model was successfully built with oligo-state as monomer and the sequence similarity is 98.6%.

**Table 4.4:** The model of Alpha-MMC with given data of oligo-state, QMEAN score and Ligand. Alpha-MMC used as template used to build the three dimensional structure of protein (<https://swissmodel.expasy.org/>).

Model#01	Built with	Oligo-state	Ligands	QMEAN score
	ProMod3 Version 1.1.0.	Monomer	1 x NCA: NICOTINAMIDE	0.14

**Table 4.5:** The pseudo-energies of the predicted balsamin model with their Z score energy (<https://swissmodel.expasy.org/>).

Scoring functional term	Z-score
C_beta interaction energy	-0.88
All-atom pairwise energy	-0.46
Solvation energy	0.70
Torsion angle energy	0.22
QMEAN4 score	0.14
QMEAN6 score	0.59

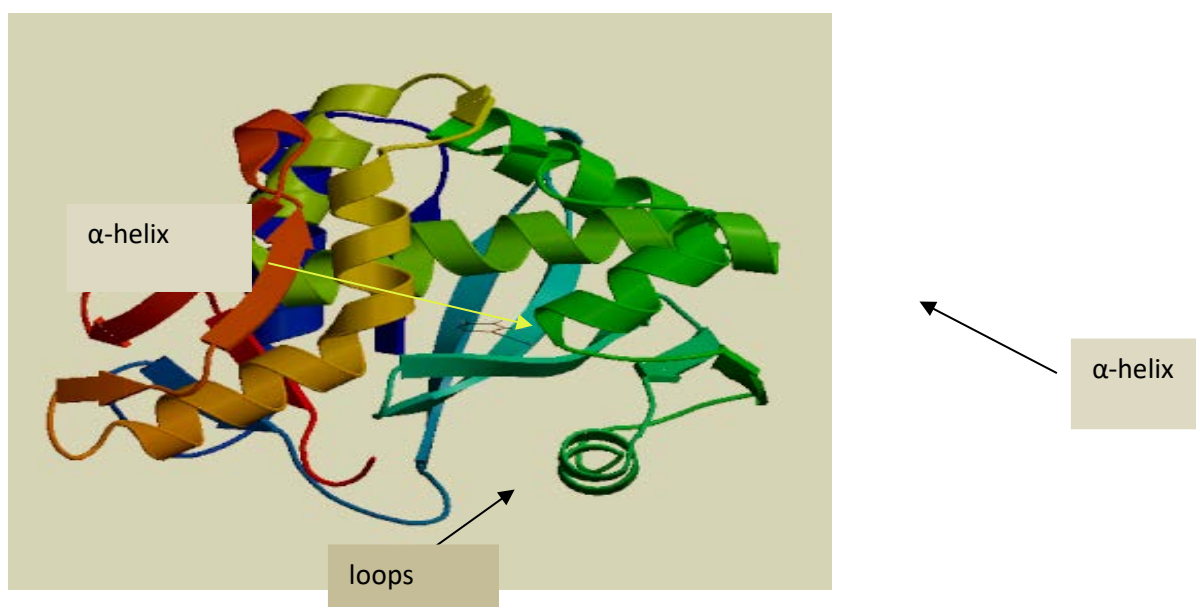


**Figure 4.8:** Predicted three dimensional structure of balsamin. Alpha-momorcharin (4yp2.1.A) as template is built with SWISS-MODEL tool (<https://swissmodel.expasy.org/>). In this model the arrangements of  $\alpha$ -helices is shown in green colour and loop regions are in red colour.

## 4.7. ASSESSMENT OF MODEL WITH RAMACHANDRAN PLOT

The model of protein was generated with SWISS-MODEL, after that it is important to validate the model of protein with two parameters: first is with accuracy of the structure and second are geometric/chemical values of the model.

It is important that the quality of the model can be expected to relate with the percentage of sequence identity between the target and the template. The different percentage of the accuracy describes their stability such as high (50% sequence identity), medium (30-50%) and low (below 30%) accuracy. It is also very important to consider the physio-chemical and geometrical parameters from Ramachandran plot of the structure of protein.

The predicted three dimensional structure of balsamin was analysed with PROCHECK tool. PROCHECK was a stereo chemical quality tool which was used to analyse the quality of protein structure and producing the number of PostScript plot with the residue-by-residue geometry. In the Ramachandran plot, each residue of the protein had two torsional angles phi and psi which depicts the backbone conformation of the balsamin (Figure 4.9). In a polypeptide the main chains N-C $\alpha$  and C $\alpha$ -C bonds relatively are free to rotate which represented by the torsion angles phi and psi, respectively. The Ramachandran plot obtained for balsamin indicated that 86.9% of the amino acids had favourable regions. Moreover PROCHECK validated balsamin model was of higher quality in terms of protein folding.

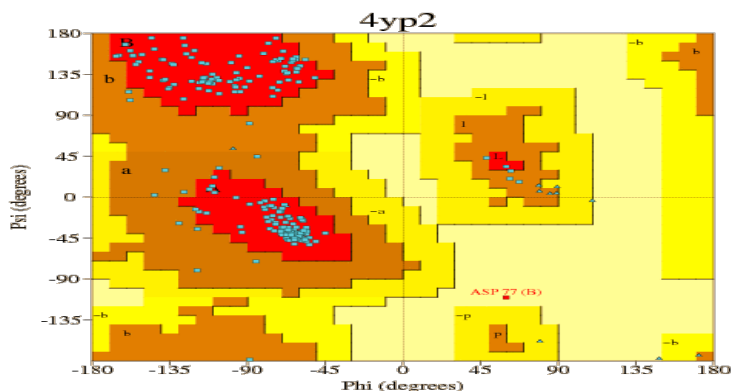


**Figure 4.9:** Ramachandran plot of balsamin. Each residue of the protein has two torsional angles phi and psi which depicts the backbone conformation of the balsamin (<http://mordred.bioc.cam.ac.uk/~rapper/rampage.php>).

## 4.8 DISCUSSION

Ribosome-inactivating proteins (RIPs) have the ability to cleave the N-glycosidic bond of adenine at particular Sarcin/ricin (SR) loop of rRNA. Ribosome-inactivating proteins have been identified into three classes according to their physical properties. Type-1 RIPs has a single chain with molecular weight of 30 kDa. Type-2 RIPs are heterodimeric proteins. Type-3 RIPs are produced inactive single polypeptide precursors. The first crystal structure of balsamin from *Momordica balsamina* was described by (Kushwaha et al., 2012a). They found the first crystal structure of type-1 RIPs which demonstrates that the slow conversion of DNA substrate by RIPs can be trapped during crystallization (Kushwaha et al., 2013).

The biological activities of RIPs are anticancer, immunosuppressive, antiviral, anti-insecticidal, antifungal and anti-human immunodeficiency virus (anti-HIV). It is proven that balsamin has anti-tumor activity from the study by (Aji et al., 2017). Two different cancer cell lines were used during her study and she investigates the possible effects of balsamin on the two key hallmarks of cancer. Firstly, the induction of apoptosis in human breast cancer MCF-7 and BT549 cells demonstrated that balsamin-induced apoptosis involved increases in caspase-3 and caspase-8 activity, upregulation of Bax, Bid, and Bad, and downregulation of BCL-2 and BCL-XL (Aji et al., 2017). Moreover, balsamin inhibited the proliferation of breast cancer cells in a dose-dependent manner with IC<sub>50</sub> values of 24.53 and 32.79 µg/ml for MCF-7 and BT549 cells, respectively. In addition,

flow cytometric analysis revealed that balsamin induced S-/G-phase cell cycle arrest (Ajji et al., 2017).

As a result, most of the ribosome-inactivating proteins literature includes the characterization of ribosome-inactivating proteins plants which can be helpful for the treatment of cancer, viral infections. Majority of RIPs have been found in the plant kingdom and investigated for their potential enzymatic and biological activities for example, trichosanthin from *Trichosanthes kirilowii*, bryodin from *bryonia dioica*, momorcharin and MAP30 from *Momordica charantia*.

*Momordica balsamina* is a plant which is found in Northern Territory in Australia and available in the markets as bitter melon. All parts of this plant such as seeds, leaves, bark as well as the fruit contain various types of nutritional and medicinal components such as alkaloids, saponins, flavonoids, terpene and balsamin protein. The leaves of this plant used as a source of nutrient because they contain 17 amino acids while mineral composition such as magnesium, phosphorus, calcium, zinc, sodium, potassium etc. It also plays an important role in pharmaceuticals and most of the components of this plant are used as anti-cancer agents.

Balsamin was purified from the seeds of *Momordica balsamina* with various biochemical techniques. Balsamin was purified employing ammonium sulphate precipitation and ion-exchange chromatography (CM-Sepharose). During the process of ammonium sulphate precipitation, most of the protein was precipitated at 60% ammonium sulphate precipitation. Balsamin has highest yield during 60% ammonium sulphate precipitation however, 20% ammonium sulphate precipitation has the lowest yield of balsamin. After the precipitation the sample was centrifuge and pellet of the protein was collected. The pellet was then dissolved in 50 mL of 10 mM phosphate buffer (pH 6.5) and dialyzed against the same buffer (10mM phosphate buffer). After the dialyzed process, balsamin was subjected to ion-exchange chromatography. One major peak (BI) and three minor peaks (BII, BIII AND BIV) were obtained with NaCl linear gradient. The further purification of balsamin will be done with gel filtration chromatography. The purified balsamin will be helps to characterize of their biological acitivities.

Qiagen PCR purification kit was used to determine the DNase-like activity of balsamin. PEGFP (+) plasmid was used with various concentration of purified balsamin from ion-exchange chromatography. Treatment of balsamin with plasmid was showed the conversion of supercoiled

DNA into linear form as visualized on agarose gel. Balsamin converted from supercoiled DNA. The lower concentration of balsamin did not shows any changes in DNA conformation and with the increased concentration of balsamin, the open circular DNA band gradually appeared. This biological activity enhances its importance and potential for disease treatment, as damage to the nucleic acid would suppress transcription and translation within the cells, ultimately promotes cell death. This approach could restrict the growth of cancer cells.

PDB BLAST analysis of balsamin indicated that balsamin has highest similarity with  $\alpha$ -MMC. SWISS-MODEL server used to predict the structure of balsamin with alpha-MMC as a template. The model of protein was successfully built as monomer. This predicted structure of balsamin was analysed by the PROCHECK server as 98.6% residues are falling in generously allowed categories.

# **Conclusion and future prospective:**

## **CONCLUSION**

Balsamin was purified from the seeds of *Momordica balsamina* through various techniques. Initially, balsamin was purified using 60% ammonium sulphate precipitation then the collected pellet was re-suspended in 10 mM phosphate buffer at pH 6.5. The protein sample was dialyzed against the same buffer then passed through ion-exchange chromatography. CM-Sepharose (weak cation exchanger) was used in ion-exchange chromatography technique. From the ion-exchange chromatography, major peaks which contained balsamin were obtained with a lower concentration of NaCl linear gradient. The fractions had balsamin were identified with SDS-PAGE gel electrophoresis. The purified fractions contained balsamin were pooled.

Alpha MMC (RIP1\_MOMCH) was used as a template to make the 3D structure of balsamin as monomer with the SWISS-MODEL server then to verify the model of balsamin a Ramachandran plot was made through PROCHECK.

In this study, balsamin was purified from the seeds of *Momordica balsamina* unfortunately, it didnot shown possess DNase-like activity due to the partial purification. The purified balsamin will be showed DNase-like activity and this biological activity can be enhanced its importance and potential for disease treatment. Further purification of balsamin will be done with gel filtration chromatography (Superdex 75). The purified balsamin will helps for the characterization of its biological activities.

## **FUTURE DIRECTION**

1. Evaluate cytotoxicity of balsamin against the tumour cell lines
2. Delivery of purified balsamin to the target cell through nanotechnology pathway.

Breast cancer deaths are increasing day-by-day worldwide, and this molecule may be used to address management of this disease through complementary and alternative medicine pathway.

Nanotechnology is an advance technology to overcome the drug delivery problems. It will help in the reduction in dosage frequency, reduces the adverse effects, and helps to maintain the plasma concentration of the drug with the average range of therapeutic drugs. The nano-particles are used for the protection of encapsulation of therapeutic drug during the process of degradation in human

GI (gastrointestinal tract) so that it can help to reach the drug to the target organ. This may be used for delivering proteins to the target site.

# References:

## References:

- A.M.R., G., L., B., F., S. & R.R.D., C. 1990. Effects of ribosome inactivating proteins on insect development – differences between Lepidoptera and Coleoptera. *Entomologia Experimentalis et Applicata*, 54, 43-51.
- ABU-DARWISH, M. S. & EFFERTH, T. 2018. Medicinal Plants from Near East for Cancer Therapy. *Frontiers in Pharmacology*, 9.
- ADRIANO, D. C. 1989. *Acidic Precipitation Case Studies*, New York, NY : Springer New York.
- AJJI, P. K., BINDER, M. J., WALDER, K. & PURI, M. 2017. Balsamin induces apoptosis in breast cancer cells via DNA fragmentation and cell cycle arrest. *Molecular and Cellular Biochemistry*, 432, 189-198.
- AJJI, P. K., SONKAR, S. P., WALDER, K. & PURI, M. 2018. Purification and functional characterization of recombinant balsamin, a ribosome-inactivating protein from *Momordica balsamina*. *International Journal of Biological Macromolecules*, 114, 226-234.
- AJJI, P. K., WALDER, K. & PURI, M. 2016. Functional Analysis of a Type-I Ribosome Inactivating Protein Balsamin from *Momordica balsamina* with Anti-Microbial and DNase Activity. *Plant Foods for Human Nutrition*, 71, 265-271.
- AKKOUH, O., NG, T., CHEUNG, R., WONG, J., PAN, W., NG, C., SHA, O., SHAW, P. & CHAN, W. 2015. Biological activities of ribosome-inactivating proteins and their possible applications as antimicrobial, anticancer, and anti-pest agents and in neuroscience research. *Applied Microbiology and Biotechnology*, 99, 9847-9863.
- ALI, A., SABINE, M.-N. & NESSAR, A. 2016. Antiglycation and Antioxidant Properties of *Momordica charantia*. *PLoS ONE*, 11, e0159985.
- AYRLE, H., MEVISSSEN, M., KASKE, M., NATHUES, H., GRUETZNER, N., MELZIG, M. & WALKENHORST, M. 2016. Medicinal plants - prophylactic and therapeutic options for gastrointestinal and respiratory diseases in calves and piglets? A systematic review. *BMC Vet. Res.*
- BAKHSHI, M., EBRAHIMI, F., NAZARIAN, S., ZARGAN, J., BEHZADI, F. & GARIZ, D. S. 2017. Nano-encapsulation of chicken immunoglobulin (IgY) in sodium alginate nanoparticles: In vitro characterization. *Biologicals*.
- BANDEHPOUR, M., YARIAN, F. & AHANGARZADEH, S. 2017. Bioinformatics evaluation of novel ribosome display-selected single chain variable fragment (scFv) structure with factor H binding protein through docking. *Journal of Theoretical and Computational Chemistry*, 16, <xocs:firstpage xmlns:xocs=""/>.
- BARBIERI, L., POLITO, L., BOLOGNESI, A., CIANI, M., PELOSI, E., FARINI, V., JHA, A. K., SHARMA, N., VIVANCO, J. M., CHAMBERY, A., PARENTE, A. & STIRPE, F. 2006. Ribosome-inactivating proteins in edible plants and purification and characterization of a new ribosome-inactivating protein from *Cucurbita moschata*. *BBA - General Subjects*, 1760, 783-792.
- BERTHOLDO-VARGAS, L. R., MARTINS, J. N., BORDIN, D., SALVADOR, M., SCHAFER, A. E., BARROS, N. M. D., BARBIERI, L., STIRPE, F. & CARLINI, C. R. 2009. Type I ribosome-inactivating proteins—Entomotoxic, oxidative and genotoxic action on *Anticarsia gemmatalis* (Hübner) and *Spodoptera frugiperda* (J.E. Smith) (Lepidoptera: Noctuidae). *Journal of Insect Physiology*, 55, 51-58.

- BIAN, X., SHEN, F., CHEN, Y., WANG, B., DENG, M. & MENG, Y. 2010. PEGylation of alpha-momorcharin: synthesis and characterization of novel anti-tumor conjugates with therapeutic potential. *Biotechnology Letters*, 32, 883-890.
- BIBI, Y., NISA, S., CHAUDHARY, F. M. & ZIA, M. 2011. Antibacterial activity of some selected medicinal plants of Pakistan.(Research article)(Report). *BMC Complementary and Alternative Medicine*, 11, 52.
- BOLOGNESI, A., BORTOLOTTI, M., MAIELLO, S., BATTELLI, M. & POLITO, L. 2016. Ribosome-Inactivating Proteins from Plants: A Historical Overview. *Molecules*, 21, 1627.
- BOLOGNESI, A., POLITO, L., OLIVIERI, F., VALBONESI, P., BARBIERI, L., BATTELLI, M. G., CARUSI, M. V., BENVENUTO, E., DEL VECCHIO BLANCO, F., DI MARO, A., PARENTE, A., DI LORETO, M. & STIRPE, F. 1997. New ribosome-inactivating proteins with polynucleotide:adenosine glycosidase and antiviral activities from *Basella rubra* L. and *Bougainvillea spectabilis* Willd. *An International Journal of Plant Biology*, 203, 422-429.
- BRADFORD, M. M. 1976. A rapid and sensitive method for the quantitation of microgram quantities of protein utilizing the principle of protein-dye binding. *Analytical Biochemistry*, 72, 248-254.
- BUYEL, J. F. 2018. Plants as sources of natural and recombinant anti-cancer agents. *Biotechnology Advances*, 36, 506-520.
- CITORES, L., IGLESIAS, R., GAY, C. & FERRERAS, J. M. 2016. Antifungal activity of the ribosome-inactivating protein BE27 from sugar beet (*Beta vulgaris* L.) against the green mould *Penicillium digitatum*. *Molecular Plant Pathology*, 17, 261-271.
- COLE, A. J., YANG, V. C. & DAVID, A. E. 2011. Cancer theranostics: the rise of targeted magnetic nanoparticles. *Trends in Biotechnology*, 29, 323-332.
- DAS, M. K., SHARMA, R. S. & MISHRA, V. 2011. A cytotoxic type-2 ribosome inactivating protein (from leafless mistletoe) lacking sugar binding activity. *International Journal of Biological Macromolecules*, 49, 1096-1103.
- DOMASHEVSKIY, A. V. & GOSS, D. J. 2015. Pokeweed Antiviral Protein, a Ribosome Inactivating Protein: Activity, Inhibition and Prospects. *Toxins*, 7, 274-298.
- ENDO, Y., MITSUI, K., MOTIZUKI, M. & TSURUGI, K. 1987. The mechanism of action of ricin and related toxic lectins on eukaryotic ribosomes. The site and the characteristics of the modification in 28 S ribosomal RNA caused by the toxins. *Journal of Biological Chemistry*, 262, 5908-5912.
- FAN, J.-M., LUO, J., XU, J., ZHU, S., ZHANG, Q., GAO, D.-F., XU, Y.-B. & ZHANG, G.-P. 2008. Effects of Recombinant MAP30 on Cell Proliferation and Apoptosis of Human Colorectal Carcinoma LoVo Cells. *Molecular Biotechnology*, 39, 79-86.
- FAN, J. M., ZHANG, Q., XU, J., ZHU, S., KE, T., GAO, D. F. & XU, Y. B. 2009. Inhibition on Hepatitis B virus in vitro of recombinant MAP30 from bitter melon. *Molecular Biology Reports*, 36, 381-388.
- FANG, E. F., ZHANG, C. Z. Y., WONG, J. H., SHEN, J. Y., LI, C. H. & NG, T. B. 2012. The MAP30 protein from bitter melon (*Momordica charantia*) seeds promotes apoptosis in liver cancer cells in vitro and in vivo. *Cancer Letters*, 324, 66-74.
- FERMANI, S., TOSI, G., FARINI, V., POLITO, L., FALINI, G., RIPAMONTI, A., BARBIERI, L., CHAMBERY, A. & BOLOGNESI, A. 2009. Structure/function studies on two type 1 ribosome inactivating proteins: Bouganin and lychnin. *Journal of Structural Biology*, 168, 278-287.

- FREDERICO, É. H. F. F., CARDOSO, A. L. B. D., MOREIRA-MARCONI, E., DE SÁ-CAPUTO, D. D. C., GUIMARÃES, C. A. S., DIONELLO, C. D. F., MOREL, D. S., PAINEIRAS-DOMINGOS, L. L., DE SOUZA, P. L., BRANDÃO-SOBRINHO-NETO, S., CARVALHO-LIMA, R. P., GUEDES-AGUIAR, E. D. O., COSTA-CAVALCANTI, R. G., KUTTER, C. R. & BERNARDO-FILHO, M. 2017. ANTI-VIRAL EFFECTS OF MEDICINAL PLANTS IN THE MANAGEMENT OF DENGUE: A SYSTEMATIC REVIEW. *African journal of traditional, complementary, and alternative medicines : AJTCAM*, 14, 33.
- GERL, R. & VAUX, D. L. 2005. Apoptosis in the development and treatment of cancer. *Carcinogenesis*, 26, 263-270.
- GIANSANTI, F., DI LEANDRO, L., KOUTRIS, I., CIALFI, A., BENEDETTI, E., LAURENTI, G., PITARI, G. & IPPOLITI, R. 2010. Ricin and Saporin: Plant Enzymes for the Research and the Clinics. *Current Chemical Biology*, 4, 99-107.
- GU, S., XUE, Q., LIU, Q., XIONG, M., WANG, W. & ZHANG, H. 2017. Erratum: Gu, S. et al. Error-Free Bypass of 7,8-dihydro-8-oxo-2'-deoxyguanosine by DNA Polymerase of *Pseudomonas aeruginosa* Phage PaP1. *Genes* 2017, 8, 18.
- HAMILTON, P. T., PENG, F., BOULANGER, M. J. & PERLMAN, S. J. 2016. A ribosome-inactivating protein in a *Drosophila* defensive symbiont. *Proceedings of the National Academy of Sciences of the United States of America*, 113, 350.
- HAMSHOU, M., SHANG, C., DE ZAEYTIJD, J., VAN DAMME, E. J. M. & SMAGGHE, G. 2017. Expression of ribosome-inactivating proteins from apple in tobacco plants results in enhanced resistance to *Spodoptera exigua*. *Journal of Asia-Pacific Entomology*, 20, 1-5.
- IGLESIAS, R., PÉREZ, Y., DE TORRE, C., FERRERAS, J. M., ANTOLÍN, P., JIMÉNEZ, P., ROJO, M. Á., MÉNDEZ, E. & GIRBÉS, T. 2005. Molecular characterization and systemic induction of single-chain ribosome-inactivating proteins (RIPs) in sugar beet (*Beta vulgaris*) leaves. *Journal of Experimental Botany*, 56, 1675-1684.
- IRVIN, J. D. 1983. Pokeweed antiviral protein. *Pharmacology and Therapeutics*, 21, 371-387.
- JONES, D. T., TAYLOR, W. R. & THORNTON, J. M. 1992. The rapid generation of mutation data matrices from protein sequences. *Computer applications in the biosciences : CABIOS*, 8, 275.
- KAUR, I., YADAV, S. K., HARIPRASAD, G., GUPTA, R. C., SRINIVASAN, A., BATRA, J. K. & PURI, M. 2012. Balsamin, a novel ribosome-inactivating protein from the seeds of Balsam apple *Momordica balsamina*. *Amino Acids*, 43, 973-981.
- KHAN, H. 2014. Medicinal plants need biological screening: a future treasure as therapeutic agents. *Biology and Medicine*, 6.
- KUMAR, M. A., TIMM, D. E., NEET, K. E., OWEN, W. G., PEUMANS, W. J. & RAO, A. G. 1993. Characterization of the lectin from the bulbs of *Eranthis hyemalis* (winter aconite) as an inhibitor of protein synthesis. *The Journal of biological chemistry*, 268, 25176.
- KUSHWAHA, G. S., PANDEY, N., SINHA, M., SINGH, S. B., KAUR, P., SHARMA, S. & SINGH, T. P. 2012a. Crystal structures of a type-1 ribosome inactivating protein from *Momordica balsamina* in the bound and unbound states. *BBA - Proteins and Proteomics*, 1824, 679-691.
- KUSHWAHA, G. S., PANDEY, N., SINHA, M., SINGH, S. B., KAUR, P., SHARMA, S. & SINGH, T. P. 2012b. Crystal structures of a type-1 ribosome inactivating protein from *Momordica balsamina* in the bound and unbound states. *Biochimica et Biophysica Acta (BBA) - Proteins and Proteomics*, 1824, 679-691.

- KUSHWAHA, G. S., YAMINI, S., KUMAR, M., SINHA, M., KAUR, P., SHARMA, S. & SINGH, T. P. 2013. First structural evidence of sequestration of mRNA cap structures by type 1 ribosome inactivating protein from *Momordica balsamina*. *Proteins: Structure, Function, and Bioinformatics*, 81, 896-905.
- LAEMMLI, U. K. 1970. Cleavage of Structural Proteins during the Assembly of the Head of Bacteriophage T4. *Nature*, 227, 680.
- LAM, S. K. & NG, T. B. 2001. Hypsin, a Novel Thermostable Ribosome-Inactivating Protein with Antifungal and Antiproliferative Activities from Fruiting Bodies of the Edible Mushroom *Hypsizigus marmoreus*. *Biochemical and Biophysical Research Communications*, 285, 1071-1075.
- LAM, Y.-H., WONG, Y.-S., WANG, B., WONG, R. N. S., YEUNG, H.-W. & SHAW, P.-C. 1996. Use of trichosanthin to reduce infection by turnip mosaic virus. *Plant Science*, 114, 111-117.
- LEE-HUANG, S., HUANG, P. L., CHEN, H.-C., HUANG, P. L., BOURINBAIAR, A., HUANG, H. I. & KUNG, H.-F. 1995. Anti-HIV and anti-tumor activities of recombinant MAP30 from bitter melon. *Gene*, 161, 151-156.
- LEUNG, S. O., YEUNG, H. W. & LEUNG, K. N. 1987. The immunosuppressive activities of two abortifacient proteins isolated from the seeds of bitter melon (*Momordica charantia*). *Immunopharmacology*, 13, 159-171.
- LOGEMANN, J., JACH, G., TOMMERUP, H., MUNDY, J. & SCHELL, J. 1992. Expression of a Barley Ribosome-Inactivating Protein Leads to Increased Fungal Protection in Transgenic Tobacco Plants. *Bio/Technology*, 10, 305.
- MAK, A. N.-S., WONG, Y.-T., AN, Y.-J., CHA, S.-S., SZE, K.-H., AU, S. W.-N., WONG, K.-B. & SHAW, P.-C. 2007. Structure-function study of maize ribosome-inactivating protein: implications for the internal inactivation region and the sole glutamate in the active site. *Nucleic Acids Research*, 35, 6259-6267.
- MANSOURI, S., CHOUDHARY, G., SARZALA, P. M., RATNER, L. & HUDAK, K. A. 2009. Suppression of Human T-cell Leukemia Virus I Gene Expression by Pokeweed Antiviral Protein. *The Journal of Biological Chemistry*, 284, 31453-31462.
- MAY, M. J., HARTLEY, M. R., ROBERTS, L. M., KRIEG, P. A., OSBORN, R. W. & LORD, J. M. 1989. Ribosome inactivation by ricin A chain: a sensitive method to assess the activity of wild-type and mutant polypeptides. *The EMBO Journal*, 8, 301-308.
- MOHANRAJ, R., RAKSHIT, J. & NOBRE, M. 2010. Anti HIV-1 and antimicrobial activity of the leaf extracts of *Calotropis procera*. *International Journal of Green Pharmacy*, 4, 242-246.
- MOLOUDIZARGARI, M., MIKAILI, P., AGHAJANSHAKERI, S., ASGHARI, M. & SHAYEGH, J. 2013. Pharmacological and therapeutic effects of *Peganum harmala* and its main alkaloids. *Pharmacognosy Reviews*, 7, 199-212.
- NARSING RAO, M. P., XIAO, M. & LI, W.-J. 2017. Fungal and Bacterial Pigments: Secondary Metabolites with Wide Applications. *Frontiers in Microbiology*, 8.
- NG, T. B., WONG, J. H. & WANG, H. 2010. Recent Progress in Research on Ribosome Inactivating Proteins. *Current Protein and Peptide Science*, 11, 37-53.
- NICOLAS, E., BEGGS, J. M., HALTIWANGER, B. M. & TARASCHI, T. F. 1997. Direct evidence for the deoxyribonuclease activity of the plant ribosome inactivating protein gelonin. *FEBS Letters*, 406, 162-164.

- OLIVIERI, F., PRASAD, V., VALBONESI, P., SRIVASTAVA, S., GHOSAL-CHOWDHURY, P., BARBIERI, L., BOLOGNESI, A. & STIRPE, F. 1996. A systemic antiviral resistance-inducing protein isolated from *Clerodendrum inerme* Gaertn. is a polynucleotide:adenosine glycosidase (ribosome-inactivating protein). *FEBS Letters*, 396, 132-134.
- PARKASH, A., NG, T. B. & TSO, W. W. 2002. Isolation and characterization of luffacylin, a ribosome inactivating peptide with anti-fungal activity from sponge gourd (*Luffa cylindrica*) seeds. *Peptides*, 23, 1019-1024.
- PIZZO, E. & DI MARO, A. 2016. A new age for biomedical applications of Ribosome Inactivating Proteins (RIPs): from bioconjugate to nanoconstructs. *Journal of Biomedical Science*, 23, 54.
- PIZZO, E., ZANFARDINO, A., DI GIUSEPPE, A. M. A., BOSSO, A., LANDI, N., RAGUCCI, S., VARCAMONTI, M., NOTOMISTA, E. & DI MARO, A. 2015. A new active antimicrobial peptide from PD-L4, a type 1 ribosome inactivating protein of *Phytolacca dioica* L.: A new function of RIPs for plant defence? *FEBS letters*, 589, 2812.
- POLITO, L., BORTOLOTTI, M., MAIELLO, S., BATTELLI, M. G. & BOLOGNESI, A. 2016. Plants Producing Ribosome-Inactivating Proteins in Traditional Medicine. *Molecules (Basel, Switzerland)*, 21.
- PUCCI, B., KASTEN, M. & GIORDANO, A. 2000. Cell Cycle and Apoptosis. *Neoplasia*, 2, 291-299.
- PURI, M., KAUR, I., KANWAR, R., GUPTA, R., CHAUHAN, A. & KANWAR, J. 2009. Ribosome inactivating proteins (RIPs) from *Momordica charantia* for anti viral therapy. *Current molecular medicine*, 9, 1080-1094.
- PURI, M., KAUR, I., PERUGINI, M. A. & GUPTA, R. C. 2012. Ribosome-inactivating proteins: current status and biomedical applications. *Drug Discovery Today*, 17, 774-783.
- ROBERTS, W. K. & STEWART, T. S. 1979. Purification and properties of a translation inhibitor from wheat germ. *Biochemistry*, 18, 2615-2621.
- SALEHI, B., KUMAR, N. V. A., ŞENER, B., SHARIFI-RAD, M., KİLİÇ, M., MAHADY, G. B., VLAISAVLJEVIC, S., IRITI, M., KOBARFARD, F., SETZER, W. N., AYATOLLAHI, S. A., ATA, A. & SHARIFI-RAD, J. 2018. Medicinal Plants Used in the Treatment of Human Immunodeficiency Virus. *International journal of molecular sciences*, 19.
- SECA, A. M. L. & PINTO, D. C. G. A. 2018. Plant Secondary Metabolites as Anticancer Agents: Successes in Clinical Trials and Therapeutic Application. *International Journal of Molecular Sciences*, 19, 263.
- SHARMA, N., PARK, S.-W., VEPACHEDU, R., BARBIERI, L., CIANI, M., STIRPE, F., SAVARY, B. J. & VIVANCO, J. M. 2004a. Isolation and characterization of an RIP (ribosome-inactivating protein)-like protein from tobacco with dual enzymatic activity. *Plant physiology*, 134, 171.
- SHARMA, N., PARK, S.-W., VEPACHEDU, R., BARBIERI, L., CIANI, M., STIRPE, F., SAVARY, B. J. & VIVANCO, J. M. 2004b. Isolation and Characterization of an RIP (Ribosome-Inactivating Protein)-Like Protein from Tobacco with Dual Enzymatic Activity. *Plant Physiology*, 134, 171-181.
- SHU, S.-H., XIE, G.-Z., GUO, X.-L. & WANG, M. 2009. Purification and characterization of a novel ribosome-inactivating protein from seeds of *Trichosanthes kirilowii* Maxim. *Protein Expression and Purification*, 67, 120-125.
- SRIVASTAVA, A., TRIVEDI, S., KRISHNA, S., VERMA, H. & PRASAD, V. 2009. Suppression of Papaya ringspot virus infection in *Carica papaya* with CAP-34, a systemic

- antiviral resistance inducing protein from *Clerodendrum aculeatum*. *Published in cooperation with the European Foundation for Plant Pathology*, 123, 241-246.
- SRIVASTAVA, S., VERMA, H. N., SRIVASTAVA, A. & PRASAD, V. 2015. BDP-30, a systemic resistance inducer from *Boerhaavia diffusa* L., suppresses TMV infection, and displays homology with ribosome-inactivating proteins. *Published by the Indian Academy of Sciences*, 40, 125-135.
- STIRPE, F., BARBIERI, L., BATTELLI, M. G., SORIA, M. & LAPPI, D. A. 1992. Ribosome-Inactivating Proteins from Plants: Present Status and Future Prospects. *Nat Biotech*, 10, 405-412.
- TAMURA, K., STECHER, G., PETERSON, D., FILIPSKI, A. & KUMAR, S. 2013. MEGA6: Molecular Evolutionary Genetics Analysis Version 6.0.
- VEERESHAM, C. 2012. Natural products derived from plants as a source of drugs. *Journal of Advanced Pharmaceutical Technology & Research*, 3, 200-201.
- VEPACHEDU, R., BAIS, H. & VIVANCO, J. 2003. Molecular characterization and post-transcriptional regulation of ME1, a type-I ribosome-inactivating protein from *Mirabilis expansa*. *An International Journal of Plant Biology*, 217, 498-506.
- VITETTA, E., FULTON, R., MAY, R., TILL, M. & UHR, J. 1987. Redesigning nature's poisons to create anti-tumor reagents. *Science*, 238, 1098-1104.
- VIVANCO, J. M., SAVARY, B. J. & FLORES, H. E. 1999. Characterization of Two Novel Type I Ribosome-Inactivating Proteins from the Storage Roots of the Andean Crop *Mirabilis expansa*. *Plant Physiology*, 119, 1447-1456.
- WANG, S., LI, Z., LI, S., DI, R., HO, C.-T. & YANG, G. 2016. Ribosome-inactivating proteins (RIPs) and their important health promoting property. *RSC Advances*, 6, 46794-46805.
- WANG, S., ZHANG, Y., LIU, H., HE, Y., YAN, J., WU, Z. & DING, Y. 2012a. Molecular cloning and functional analysis of a recombinant ribosome-inactivating protein (alpha-momorcharin) from *Momordica charantia*. *Applied Microbiology and Biotechnology*, 96, 939-950.
- WANG, S., ZHANG, Y., LIU, H., HE, Y., YAN, J., WU, Z. & DING, Y. 2012b. Molecular cloning and functional analysis of a recombinant ribosome-inactivating protein (alpha-momorcharin) from *Momordica charantia*. (BIOTECHNOLOGICALLY RELEVANT ENZYMES AND PROTEINS). *Applied Microbiology and Biotechnology*, 96, 939.
- WANG, Y.-X., NEAMATI, N., JACOB, J., PALMER, I., STAHL, S. J., KAUFMAN, J. D., HUANG, P. L., HUANG, P. L., WINSLOW, H. E., POMMIER, Y., WINGFIELD, P. T., LEE-HUANG, S., BAX, A. & TORCHIA, D. A. 1999. Solution Structure of Anti-HIV-1 and Anti-Tumor Protein MAP30: Structural Insights into Its Multiple Functions. *Cell*, 99, 433-442.
- WONG, J., NG, T., CHEUNG, R., YE, X., WANG, H., LAM, S., LIN, P., CHAN, Y., FANG, E., NGAI, P., XIA, L., JIANG, Y. & LIU, F. 2010. Proteins with antifungal properties and other medicinal applications from plants and mushrooms. *Applied Microbiology and Biotechnology*, 87, 1221-1235.
- XIONG, S., YU, K., LIU, X., YIN, L., KIRSCHENBAUM, A., YAO, S., NARLA, G., DIFEO, A., WU, J. & YUAN, Y. 2009. Ribosome-inactivating proteins isolated from dietary bitter melon induce apoptosis and inhibit histone deacetylase-1 selectively in premalignant and malignant prostate cancer cells. *Int. J. Cancer* 2009; 125: 774-782. When the article cited above published online in the formatted version, the necessary grant sponsor and number

- information had been omitted. The opening page footnote should have read. *Int. J. Cancer*, 125, 1995.
- YAMINI, S., PANDEY, S. N., KAUR, P., SHARMA, S. & SINGH, T. P. 2015. Binding and structural studies of the complexes of type 1 ribosome inactivating protein from *Momordica balsamina* with cytosine, cytidine, and cytidine diphosphate. *Biochemistry and Biophysics Reports*, 4, 134-140.
- ZENG, M., ZHENG, M., LU, D., WANG, J., JIANG, W. & SHA, O. 2015. Anti-tumor activities and apoptotic mechanism of ribosome-inactivating proteins. *Chinese Journal of Cancer*, 34, 30.
- ZHANG, F., LIN, L. & XIE, J. 2016. A mini-review of chemical and biological properties of polysaccharides from *Momordica charantia*. *International Journal of Biological Macromolecules*, 92, 246-253.
- ZHANG, Y.-B., LIU, H., ZHU, C.-Y., ZHANG, M.-X., LI, Y.-L., LING, B. & WANG, G.-C. 2014. Cucurbitane-type triterpenoids from the leaves of *Momordica charantia*. *Journal of Asian Natural Products Research*, 16, 1-6.
- ZHU, F., ZHANG, P., MENG, Y.-F., XU, F., ZHANG, D.-W., CHENG, J., LIN, H.-H. & XI, D.-H. 2013. Alpha-momorcharin, a RIP produced by bitter melon, enhances defense response in tobacco plants against diverse plant viruses and shows antifungal activity in vitro.(Report). *Planta*, 237, 77.
- ZHU, F., ZHOU, Y.-K., JI, Z.-L. & CHEN, X.-R. 2018. The Plant Ribosome-Inactivating Proteins Play Important Roles in Defense against Pathogens and Insect Pest Attacks.(Report)(Author abstract). *Frontiers in Plant Science*, 9.
- ZOUBENKO, O., HUDAK, K. & TUMER, N. 2000. A non-toxic pokeweed antiviral protein mutant inhibits pathogen infection via a novel salicylic acid-independent pathway. *An International Journal on Molecular Biology, Molecular Genetics and Biochemistry*, 44, 219-229.

# Appendix:

## PROTEIN ESTIMATION

The protein concentration is determined by Bradford assay. Bovine serum albumin is used as a standard with concentration 1 mg/ml to 0.0625 mg/ml. The standard curve from Bradford assay

result shows in figure 3.3.1 is used to determine the concentration of protein as the results are shows in materials and methods.

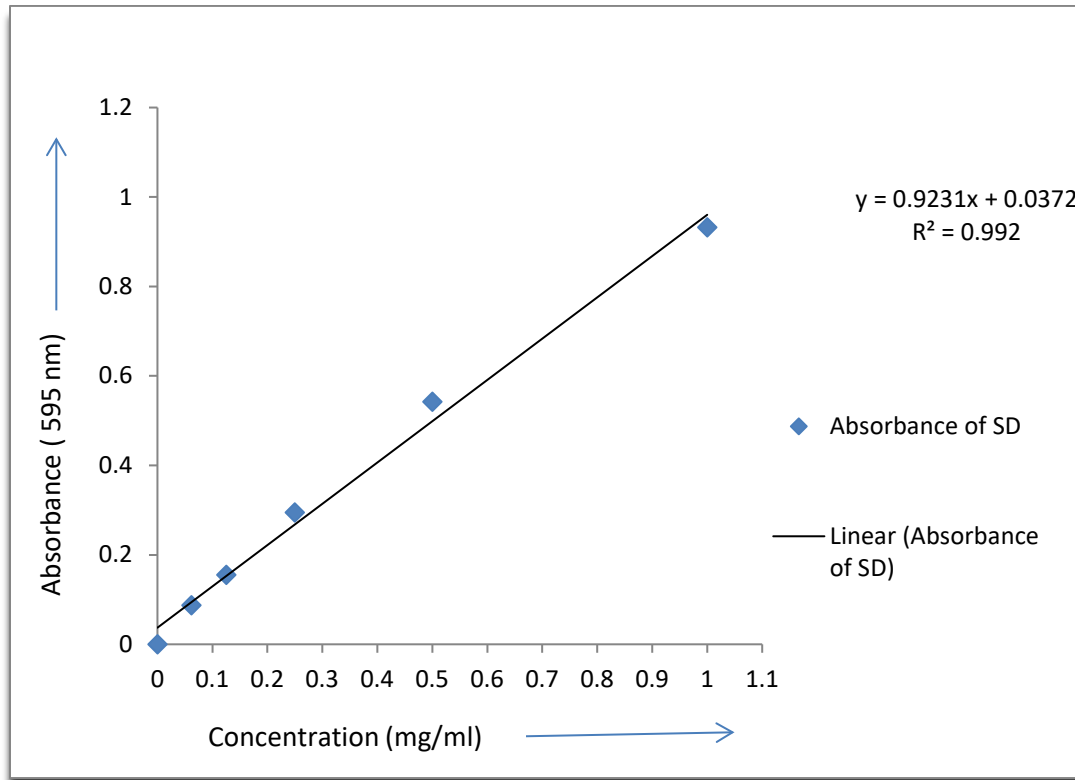


**Figure 3.2.1.1:** Standard curve of protein.

### 3.2.2.1: PROTEIN CONCENTRATION CALCULATIONS:

**Table 3.4:** The concentration of protein of ammonium sulphate precipitation was performed with Bradford assay and the standard curve was used to determine the yield of protein in each sample. The 60% ammonium precipitation has the highest protein yield however the 20% has the lowest protein yield.

Concentration of protein (mg/ml)	Protein yield (%)
Crude sample of protein (1.438)	100
20% Ammonium precipitation (0.282)	18.45
40% (after 20%) Ammonium precipitation (0.832)	59.89
60% (after 20% to 40%) Ammonium precipitation (0.545)	38.26
40% Ammonium precipitation (0.832)	59.89
60% (after 40%) Ammonium precipitation (0.949)	68.7
60% Ammonium precipitation (1.225)	89.49

**Table 3.5:** List of bioinformatics tools used in this project

Name of software/program	Application name	Source
BLAST	Search Sequence similarity	<a href="http://www.ncbi.nlm.nih.gov/blast">http://www.ncbi.nlm.nih.gov/blast</a>
Clustal X2	Multiple alignment	<a href="http://www.ebi.ac.uk/clustalX2">http://www.ebi.ac.uk/clustalX2</a>
PROTPARAM	Biochemical parameters of protein	<a href="http://www.expasy.ch/protparam">http://www.expasy.ch/protparam</a>
SWISS-MODEL	Protein structure	<a href="http://www.expasy.ch/swissmodel">http://www.expasy.ch/swissmodel</a>
PROCHECK	To validate the protein structure	<a href="http://www.ebi.ac.uk/thorntonsrv/software/PROCHECK">http://www.ebi.ac.uk/thorntonsrv/software/PROCHECK</a>

**Table 3.1:** The concentrations of reagents were used to prepare the 12% separating gel

Name of reagent	Concentration of reagent ( $\mu$ l)
1.5 mM HCL (8.8)	1250
10% Ammonium persulfate	50
30% Acrylamide solution	1660
10% SDS	50
MilliQ water	2082
TEMED	5

**Table 3.2:** The concentrations of reagents were used to prepare 4% stacking gel.

<b>Name of the reagent</b>	<b>Concentration of reagent (<math>\mu</math>l)</b>
0.5 mM HCL buffer (6.8)	1000
30% Acrylamide solution	670
10% Ammonium persulfate	50
10% SDS	50
MilliQ water	2298
TEMED	5

**Table 4.3:** List of amino acids present in each species of ribosome-inactivating protein

Name of protein/amino acids	Bryodin	$\alpha$ -MMC (momorcharin)	balsamin	Trichomislin	Trichobakin	B – Luffin	Trichosanthos	Average
Ala	10.88	8.74	9.5	11.85	10.72	10.43	11.33	10.47
Cys	0	0	0	0	0.34	0	0	0.053
Asp	3.22	4.54	4.94	2.96	4.49	3.59	3.64	3.93
Glu	4.43	3.84	4.18	4.07	3.80	4.31	4.04	4.09
Phe	3.62	4.54	3.42	4.07	4.15	5.75	3.64	4.19
Gly	4.83	6.99	6.46	4.44	4.84	4.67	4.45	5.26
His	0.40	1.04	1.14	0	0.34	0.71	0.40	0.58
Ile	7.25	7.69	7.22	8.51	7.26	8.99	7.69	7.81
Lys	4.83	3.84	3.80	4.44	3.46	6.83	4.45	4.51
Leu	1.048	11.18	10.64	12.22	11.07	9.35	0.71	10.68
Met	0.80	1.39	1.14	1.11	2.42	1.43	1.21	1.38
Asn	7.25	5.59	6.08	7.03	5.88	6.83	7.28	6.53
Pro	2.82	3.84	4.18	2.96	3.46	3.59	3.64	3.50
Gln	3.22	3.84	4.18	3.70	3.80	3.59	4.04	3.77
4.83	5.94	6.08	4.81	4.84	4.84	3.59	5.26	5.05
Ser	10.48	8.74	7.98	10	10.03	10.07	9.71	9.56
Thr	7.66	6.29	6.84	5.55	7.26	5.75	6.88	6.59
Val	6.85	6.64	6.08	6.29	6.57	6.11	6.47	6.43
Trp	0.40	0.34	0.38	0.37	0.34	0.35	0.30	0.37
Tyr	5.64	4.89	5.70	5.55	4.84	3.95	5.66	5.15
Total	248	286	263	270	289	278	247	268.7